An Approach For Shaped-Beam Pattern Synthesis With Spherical Antenna Array

Arpit Kumar Baranwal

Department of Electrical Engineering
National Institute of Technology,Rourkela
Rourkela-769008, Odisha, INDIA

May 2014

An Approach For Shaped-Beam Pattern Synthesis With Spherical Antenna Array

A thesis submitted in partial fulfillment of the
requirements for the degree of

Master of Technology

in

Electrical Engineering

by

Arpit Kumar Baranwal
(Roll-212EE1203)

Under the Guidance of

Prof.K. R. Subhashini

Department of Electrical Engineering
National Institute of Technology,Rourkela
Rourkela-769008, Odisha, INDIA
2012-2014

Department of Electrical Engineering

National Institute of Technology, Rourkela

C E R T I F I C A T E

This is to certify that the thesis entitled ***"An Approach For Shaped-Beam Pattern Synthesis With Spherical Antenna Array"*** *by* ***Mr. Arpit Kumar Baranwal****, submitted to the National Institute of Technology, Rourkela (Deemed University) for the award of Master of Technology in Electrical Engineering, is a record of bonafide research work carried out by him in the Department of Electrical Engineering , under my supervision. I believe that this thesis fulfills the requirements for the award of degree of Master of Technology.The results embodied in the thesis have not been submitted for the award of any other degree elsewhere.*

Prof.K. R. Subhashini

Place:Rourkela

Date:

To My Loving parents and Inspiring GUIDE

Acknowledgements

First and foremost, I am truly indebted to my supervisor Professor K. R. Subhashini for their inspiration, excellent guidance and unwavering confidence through my study, without which this thesis would not be in its present form. I also thank her for all the gracious encouragement throughout the work.

I express my gratitude to the members of Masters Scrutiny Committee, "Professors D. Patra, S. Das, P. K. Sahoo, Supratim Gupta" for their advise and care. I am also very much obliged to Head of the Department of Electrical Engineering, NIT Rourkela for providing all the possible facilities towards this work. I also thanks to other faculty members in the department for their invaluable support.

I would like to thank my colleagues "Joshi Katta, Surendra Kumar Bairwa, Pawan Kumar, A T Praveen Kumar, D Suneel Varma", for their enjoyable and helpful company I had with them.

My wholehearted gratitude to my parents, "Vijay Kumar Baranwal and Seema Baranwal' and my grandfather "Sadanand Baranwal" for their invaluable encouragement and support.

ARPIT KUMAR BARANWAL
Rourkela, MAY 2014

Contents

Abstract

A modern high-speed aircraft will be installed with multiple antennas protruded from its structure for communication purpose, navigation, Instrumental Landing System etc. There may be more than 25 antennas that can cause considerable amount of drag that will ultimately affect the efficiency of aircraft. Nowadays, integration of these antenna on the surface of the aircraft is very much required and important. Need of these antenna will be more pronounced when large-aperture antennas are required in applications like military airborne radars,satellite communication etc. In this work, spherical shaped antenna array has been proposed and discussed in details with consideration of mutual coupling. Further, proposed spherical array has been utilized to generate Shaped-patterns. Radiation patterns like Cosecant-squared shaped pattern which are significantly applied in radar and navigation applications is generated using DE & SSO optimization techniques and compared with conventional arrays. Further, the work is extended to a newly designed shape of Indian geographical boundary-line with the proposed spherical array. Besides simulation results, to have a practical understanding of its radiation pattern, spherical array is modelled with patch dipole in Computer Simulation Technology(CST) software and is processed to obtain all the important parameters like Polar & 3D far field Radiation pattern, Side Lobe Level, Beam-width, S-parameters, E-field & H-field patterns, current-density etc.

List of Figures

List of Tables

List of Abbreviations

Abbreviation	Description
AF	Array Factor
DE	Differential Evolution
SSO	Simplified Swarm Optimization
PSO	Particle Swarm Optimization
lin	Linear
plan	Planar
cir	Circular
sph	Spherical
mut	Mutual Coupling
des	Desired
rand	Random
CSC	Cosecant-squared pattern
GUI	Graphical User Interface
MLL	Main Lobe Level
SLL	Side Lobe Level
HPBW	Half-Power Beamwidth
CST	Computer Simulation Technology
TS	Transient Solver
FMS	Frequency Domain Solver
IES	Integral Equation Solver
ES	Eigenmode Solver

Chapter 1

INTRODUCTION

1.1 Introduction

Antenna designers always keep on devising new and advanced techniques to improve the existing designs and introduce new antenna models to achieve better radiation characteristics at reduced cost, size and weight. In recent scenario, conformal arrays [1] has a very tremendous impact in the field of antennas, as they conforms the prescribed shape. The prescribed shape might be a part of an aircraft, high-speed trains etc which consist of more than 25 different types of antennas for their communication systems and navigation system. Use of conventional antenna array results in severe drag which limits the efficiency in these applications. On the other hand, conformal arrays easily gets integrated with different structures without any introduction of extra drag. In this thesis, spherical array antenna has been modelled, formulated and extensively employed with Differential Evolution(DE) and Simple Swarm Optimization(SSO) techniques to generate the desired Shaped patterns. As spherical array comprising of isotropic antenna elements has nearly omni-directional radiation pattern, so it can be easily utilized to generate the required adaptive radiation patterns with the efficient use of signal-processing and beam-steering processes.

1.2 Literature Review

Antenna arrays are becoming a very important component of modern communication system because of the exhaustive technological improvement in this field and rapidly rising requirements. To meet the current trend, antenna system must be efficient in its operation with high accuracy. The concept of antenna arrays [2] and detailed analysis of this field of work is very much important for the new research proposals in this area. Basic array formation[2, 19], their characteristics and area of applications are required to have better understanding about antenna systems. Conformal arrays [1], which is an important area of research in present scenario has been studied in details. Mutual coupling, factors responsible for it and its consequences on basic antenna arrays has been studied [5, 6] and applied on proposed array [7, 4, 3]. Various optimization algorithms, their classification [11] and importance based on the requirements and desired constraints has been reviewed in details. Evolutionary algorithm "DE" [13, 20, 12] and nature-inspired optimization "SSO" [15, 16] that can be used efficiently in multi-objective function are referred in details along with their application methodology [14, 21]. The Cosecant-shaped beam formation [8] and their implementation with linear [10] and circular [9] arrays has been thoroughly studied and utilized in the present work. Further, CST modelling of patch dipole [18] as radiating element has been studied for proposed spherical array.

1.3 Objectives

This thesis work consist of the following objectives as mentioned below:

- Modelling and formulation of Array Factor of the proposed spherical antenna array using the concepts of basic antenna arrays(Linear & Circular).

- Generation of some specific shaped-radiation patterns using powerful

evolutionary and nature inspired algorithms that can be extensively utilized in the present scenario of applications.

- To study and discuss the effect of mutual coupling on various antenna arrays with its detailed procedure of computation and simulation results.

- To show the superiority of the proposed spherical array over linear and circular array with the help of the obtained simulation results.

1.4 Thesis Organization

The thesis work has been organized as follows:

- In chapter 2, a brief introduction of linear and circular antenna arrays is presented. Further, the mathematical Array Factor modelling of proposed spherical antenna array conceiving two basic existing conventional arrays(Linear & Circular) has been discussed.

- Chapter 3 discusses the concept of mutual coupling and various impact of mutual coupling. The Array factor variation from its standard form with the introduction of mutual coupling effect is formulated. Simulation is performed on the linear, planar, circular and spherical array for the newly formulated array factor to stude the consequences.

- In Chapter 4, Cosecant-Squared shaped beam has been discussed along with its applications. Synthesis of Cosecant-squared shaped radiation pattern has been carried out with the aid of DE & SSO on Linear, Circular & proposed spherical array.

- Chapter 5 portraits an attempt to mathematically model INDIA contour and making the contour as the desired radiation beam pattern. Synthesis for the generation of this contour from the spherical antenna array using DE & SSO is also presented.

- In chapter 6, CST based design of the proposed spherical array using patch dipole and strip dipole as the basic radiators of spherical array is presented. Based on Transient-solver method of simulation, their performances is shown. Further, an attempt to validate the CST designs has been done by comparing the CST results with MATLAB based results of the spherical array.

Chapter 2

ANTENNA ARRAYS

A single antenna element radiation pattern is quite wider with low value of directive gain. Thus, in many applications where better performance like higher directivity, lower side lobe level(SLL) is required, these antenna elements will not be efficiently utilized. Hence, two strategies can be followed to enhance the performance of antenna system. One way is to increase the dimensions of the single antenna elements, other way is by increasing the number of antenna elements to form an assembly of antenna system without any increase in size of its elements. This new assemble of multi-element antenna can be referred as Antenna Array. The total radiation pattern of an antenna array can be calculated by performing the vector addition of the radiation pattern of each element of the array. The total field of an array can be given as:

$$E_{total} = [E_{single\ element\ at\ reference\ point}] * [Array\ Factor]$$

Basically, there are five controlling parameters [2] that directly or indirectly affect the total radiation pattern of an array.

1. The geometrical shape of array.
2. The relative spacing between elements.
3. The excitation amplitude of each individual elements.
4. The excitation phase of each individual elements.

5. The radiation pattern of each individual elements.

2.1 LINEAR ARRAY

A linear array is an arrangement of antenna elements placed along a regular and straight line with the orientation of each element in same direction. The elements should be arranged such that each individual element radiation pattern must interfere constructively to give a desired pattern. Let a linear arrangement of 'N' isotropic elements with equal inter-element spacing 'd' placed in z-direction as shown in fig. 2.1. The array factor [2] of the linear array can be given as:

$$AF_{lin}(\theta, \phi) = \sum_{n=1}^{N} I_n * exp^{j[(n-1)kd\cos\theta+\beta]} \tag{2.1}$$

where, β is the progressive phase shift between adjacent elements
k is the propagation constant

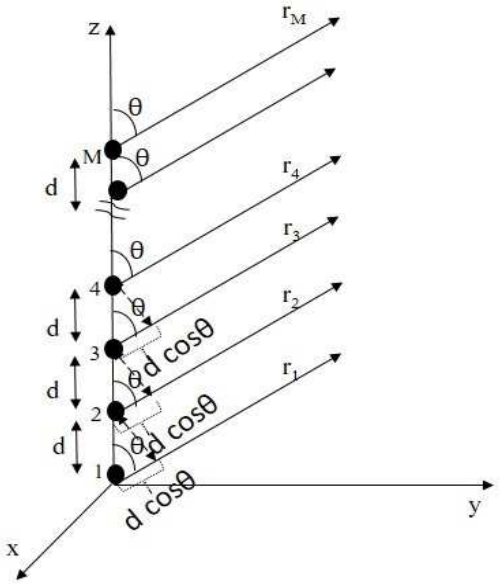

Figure 2.1: Linear Antenna Array

2.2 CIRCULAR ARRAY

A circular array is an arrangement of antenna elements along the periphery of a circle such that each individual element is excited with some amplitude and phase. Let us assume that a circular array of radius 'a' which consist of M isotropic antenna elements at equal inter-element spacing in x-y plane as shown in fig. 2.2. The array factor of the circular array [2] can be written as:

$$AF_{cir}(\theta,\phi) = \sum_{m=1}^{M} I_m * exp^{j[ka\sin\theta\cos(\phi-\phi_m)+\alpha_m]} \tag{2.2}$$

where, ϕ_m is the angular position of m_{th} element on the circle
α_m is the excitation phase of m_{th} element

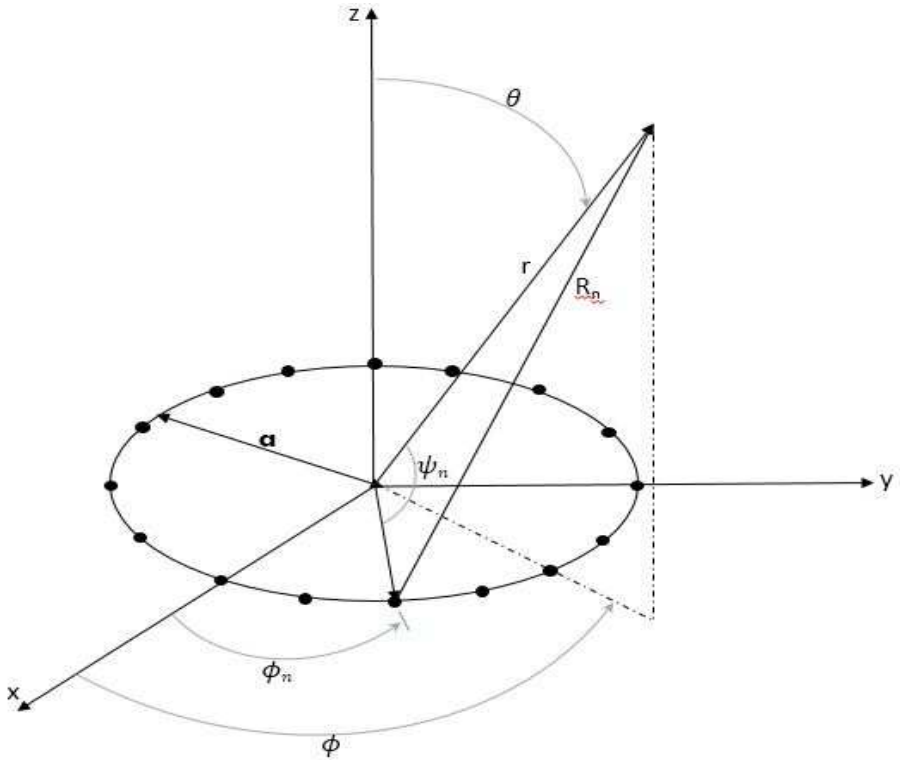

Figure 2.2: Circular Antenna Array

2.3 SPHERICAL ARRAY

Conformal arrays are specially designed arrays that conforms to a surface considering behaviours like hydrodynamic,aerodynamic etc. These arrays

with their radiating elements can be easily mounted on or integrated on the smooth curved surface thereby reducing drags and disturbances by the installed components. Spherical shaped antenna array can be treated as one of the conformal array of great interest. An attractive feature of spherical array is that, any point in far-field will see the similar environment by spherical array as its elements are placed symmetrically and thereby the radiation pattern will remain same as the considered far-field point is moved over the space. [1]. These arrays can be used to achieve multiple-beams and adaptive patterns reshaping based on its easy electronic beam steering and signal processing capabilities. Applications like Low Earth Orbiting Satellite Communication requires omni-directional nature, so that beam can be steered in both azimuthal and elevation.

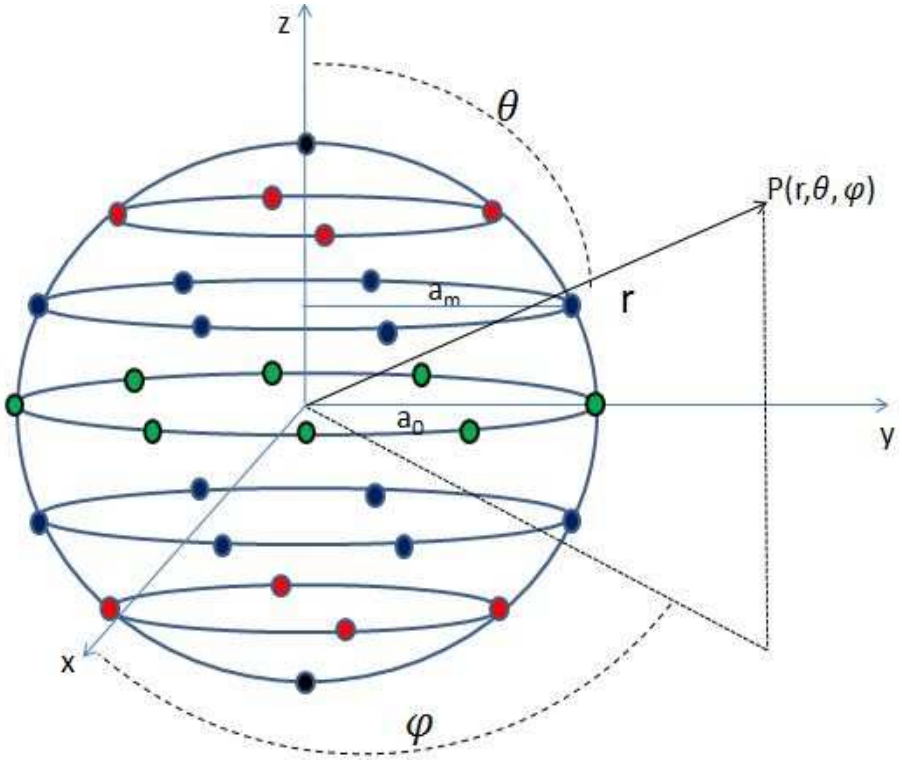

Figure 2.3: Spherical Antenna Array

2.3.1 Array Factor Formulation of Spherical Array

For modelling spherical shaped array, the geometry can be viewed as it(spherical array) is a linear stack arrangement of circular antenna array placed one above

the other such that, the radius of each progressive stacked circular array follow a definite set of rules to form a spherical shaped array as given in fig. 2.3. Here, spherical array is modelled by taking N circular array of varying radius a_n in stack with each circular array consist of M discrete and similar set of antenna elements. The array factor for n_{th} circular array of spherical array can be rewritten from 2.2 as:

$$AF(\theta, \phi) = \sum_{m=1}^{M} I_m exp^{(jka_n \sin(\theta)\cos(\phi-\phi_m)+j\psi_m)} \tag{2.3}$$

where, a_n is radius for n_{th} circular array can be calculated and given as in fig. 2.4

$$a_n = sqrt(a_0^2 - d_n^2)$$

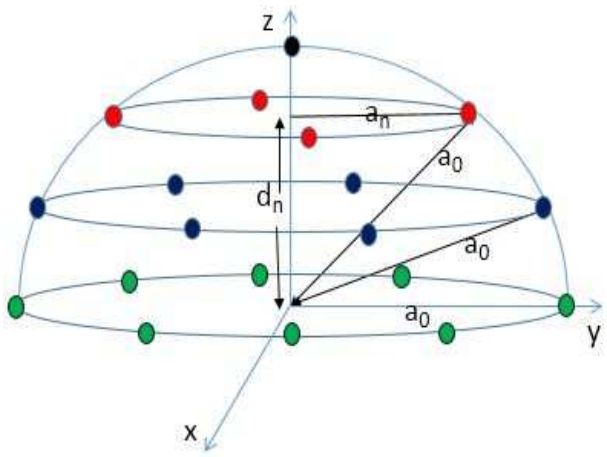

Figure 2.4: Radius of n_{th} Circle of Spherical Antenna Array

To form a spherical geometry, such circular arrays are to be arranged in a linear fashion.The linear array factor for 2N+1 antenna elements can be rewritten from **??** as:

$$AF_{lin}(\theta, \phi) = \sum_{n=-N}^{N} I_n * exp^{j[nkd\cos\theta+\beta]} \tag{2.4}$$

Hence, a spherical antenna array modelled with 2N+1 circular array stacks

can be represented by combining 2.3 & 2.4 as:

$$AF_{sph}(\theta,\phi) = \sum_{m=1}^{M} I_m exp^{(jka_n \sin(\theta)\cos(\phi-\phi_m)+j\psi_m)} * \sum_{n=-N}^{N} I_n * exp^{j[nkd_n\cos\theta+\beta]} \tag{2.5}$$

Rearranging the above equation, we have

$$AF_{sph}(\theta,\phi) = \sum_{n=-N}^{N}\sum_{m=1}^{M} I_{mn} exp^{(jka_n sin(\theta)cos(\phi-\phi_{mn})+j\psi_m)+(jkd_n cos(\theta)+\beta_n)} \tag{2.6}$$

The above defined array factor expression gives a truncated spherical array with a slice at its top and bottom surface. Hence, to form a complete spherical array, an antenna element is added both at its top and bottom surface.The final expression for the spherical array factor with 2M+1 circular array can be re-written as:

$$AF_{sph}(\theta,\phi) = \sum_{n=-N}^{N}\sum_{m=1}^{M} I_{mn} exp^{(jka_n sin(\theta)cos(\phi-\phi_{mn})+j\psi_m)+(jkd_n cos(\theta)+\beta_n)} + exp^{(jka_0\cos\theta)} + exp^{(-jka_0\cos\theta)} \tag{2.7}$$

where,

I_{mn} is the current excitation for m_{th} antenna element of n_{th} circular array,

k is the propagation constant,

θ is the elevation angle,

ϕ is the azimuth angle,

ϕ_{mn} is the azimuth position of m_{th} antenna element on n_{th} circular array,

a_n is the radius for n_{th} circle of spherical array and is given as in fig. 2.4:

$$a_n = sqrt(a_0^2 - d_n^2)$$

a_0 is the radius of spherical array,

ψ_m is the beam steering phase angle in azimuth direction,

d_n is the distance of n_{th} circular array from reference circular array at the origin,

β_n is the progressive phase shift between n_{th} and reference circular array.

Chapter 3

Mutual Coupling In Antenna Arrays

When two antennas are placed close to each other, such that they are acting as transmitter/receiver, then a portion of energy which is intended for one may affect the other. Due to this, the portion of energy incident on them may be scattered back in various directions making them to behave as secondary transmitters. This phenomenon of interchange of energy is known as "Mutual Coupling". Practically, as mutual coupling does not follow any rules or mathematical boundaries, so is difficult to calculate and only significant contribution of it can be considered.

3.1 Important Factor Responsible for Mutual Coupling

Mutual coupling between antenna depends on the following factors [2] :
a)Radiation Characteristic of each Antenna Elements: It plays an important role for mutual coupling as if the radiation pattern of an antenna element is more directive in the direction of another antenna element then electromagnetic interaction between the two increases and hence mutual coupling between them will be more significant.
b)Relative Separation between Antenna Elements: The amount of coupling depends upon the power received by the other antenna, which in turn depends upon the distance of separation. As the distance of separation increases, the effect of mutual coupling on antenna decreases and vice-versa.

Hence, it follows an inverse law with the distance of separation.
c)Relative Orientation of each Antenna Elements: Polarization is an important factor for the extent of coupling between antennas placed in proximity to each other as two cross-polarized antenna radiation pattern do not interact significantly.

3.2 Effect of Mutual Coupling

The above discussed factors influence the performance of the antenna array by varying its element impedance, reflection coefficients, and overall antenna pattern. Hence, mutual coupling effect leads to the following:
a)Degrades the radiation pattern of Antenna Array.
b)Introduces Coupling Losses.
c)Reduces Antenna Efficiency.

3.3 Computational Methods

There are three major classification [5] for the calculation of mutual coupling between antenna elements as:
1.**Classical Analysis method or Pattern multiplication method:** This method deals with the antenna arrays consisting of well-behaved elements which are identical in their configuration and are excited by same excitation amplitude and phase.
2.**Numerical techniques or Method of moment:** This method is applied for electrically large and array of dissimilar elements. It gives good level of accuracy but are difficult to apply for large arrays.In this method, a large matrix equation is created and the size of matrix increases as square of the array size.
3.**Active element pattern method:** This method is generally used in cases when both of the above method fails to apply. Active element pattern method utilizes the already measured pattern of each individual elements in the array environment. They are quite faster in their operation [5] as com-

pared to other methods.
Here in this thesis, main focus will be on classical analysis method of computation and its procedures.

3.4 Classical Analysis Method

Classical Analysis method is applied in arrays of 'well-behaved' antenna elements. The term "Well-behaved elements" refers to antenna elements which have relative distribution of current amplitude and phase unchanged from one element to other. An array of half-wave dipole elements is one of the example of such an array. The benefits of well-behaved elements array on mutual coupling is that, it will change only its active input impedance but not the shape of its current distribution. This will gives an identical element pattern for each individual elements of the array, which can be easily factored out of the total array pattern expression without introducing any significant error in the expression. However, this method fails for arrays which consist of electrically large and dissimilar elements, as the element pattern are not identical to be factored out comprehensively.

3.4.1 Mutual Impedance Calculation for Two-Element Antenna system

Consider a two-element antenna system represented by a two-port [2] network with its T-network equivalent model as shown in fig.3.2 and by voltage-current relations as:

$$V_1 = Z_{11}I_1 + Z_{12}I_2 \tag{3.1}$$

$$V_2 = Z_{21}I_1 + Z_{22}I_2 \tag{3.2}$$

where,

$$Z_{11} = \left.\frac{V_1}{I_1}\right|_{I_2=0}$$

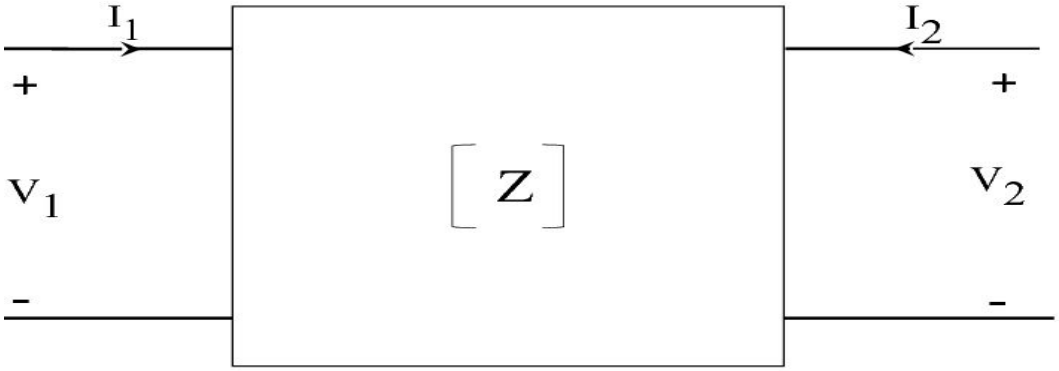

Figure 3.1: Two-port Network

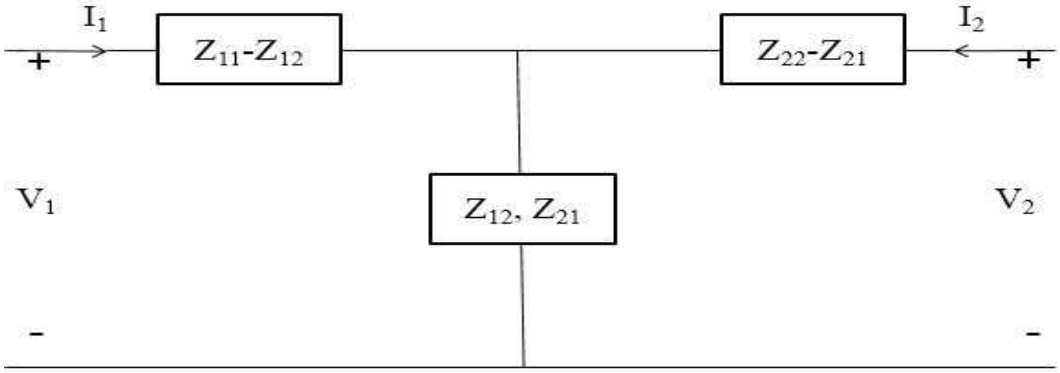

Figure 3.2: T-Network Equivalent

is the input impedance at port 1 with port 2 open-circuited,

$$Z_{12} = \left.\frac{V_1}{I_2}\right|_{I_1=0}$$

is the mutual impedance at port 1 due to current at port 2 with port 1 open-circuited,

$$Z_{21} = \left.\frac{V_2}{I_1}\right|_{I_2=0}$$

is the mutual impedance at port 2 due to current at port 1 with port 2 open-circuited,

$$Z_{22} = \left.\frac{V_2}{I_2}\right|_{I_1=0}$$

is the input impedance at port 2 with port 1 open-circuited,

Since the two antenna elements are identical, so by reciprocity theorem, we have

$$Z_{12} = Z_{21}$$

Further, the impedance Z_{11} and Z_{22} are the input impedance of antenna 1 and 2 respectively.

When both elements are radiating, the effect of one element on the other is such that it modifies the overall impedance of the antenna element and the extent of modification depends on their relative placement. Hence, equation 3.1 & 3.2 can be rewritten as:

$$Z_{1d} = \frac{V_1}{I_1} = Z_{11} + Z_{12}\left(\frac{I_2}{I_1}\right) \tag{3.3}$$

$$Z_{2d} = \frac{V_2}{I_2} = Z_{22} + Z_{21}\left(\frac{I_1}{I_2}\right) \tag{3.4}$$

where Z_{1d} and Z_{2d} are the driving point impedance which depends on the self-impedance, mutual-impedance and the current ratio. Hence, to analyse the performance of antenna array under mutual coupling environment, mutual impedance of plays an important role and need to be computed.

Now, for the calculation of mutual impedance [19], let us consider a simple 2-element dipole antenna system as shown in fig3.3.

The open-circuit voltage induced in antenna 2 due to radiation from antenna

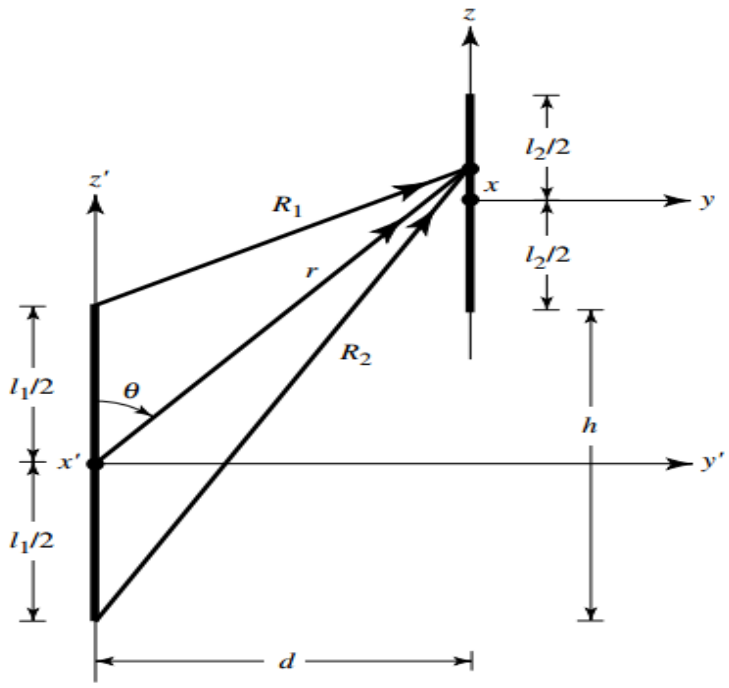

Figure 3.3: Two-element dipole antenna system

1 is given by the relation [2]:

$$V_{21} = -\frac{1}{I_2}\int_{-l_2/2}^{l_2/2} E_{z21}(z')I_2(z')dz' \tag{3.5}$$

where, $E_{z21}(z')$=E-field component radiated by antenna 1, which is parallel to antenna 2

$I_1(z')$=current distribution along antenna 1

$I_2(z')$=current distribution along antenna 2

Then, the mutual impedance referred to input current of antenna 1 can be given by the expression

$$Z_{21} = \frac{V_{21}}{I_1} = -\frac{1}{I_1 * I_2}\int_{-l_2/2}^{l_2/2} E_{z21}(z')I_2(z')dz' \tag{3.6}$$

3.4.2 Computation of Array Factor with Mutual Coupling

Soon after the computation of mutual impedance for each antenna element of an array based on the above procedure, the calculation of array radiation pattern in mutual coupling environment can be done by modelling the array excitation as a set of Thevenin equivalent voltage sources [5] with non-zero source impedances(Z_{gq}) as shown in fig3.4. Each element of this array can be modelled by thevenin equivalent circuit as shown in fig.3.3 with an extra impedance i.e. active input impedance Z_{aq} due to the effect of mutual coupling. If V_q is the feed voltage, then the resulting feed current I_q will be given by applying Kirchoff's voltage law in fig.3.5 as [6]:

$$I_q = \frac{V_q}{Z_{aq} + Z_{gq}} \tag{3.7}$$

It is clear that resulting current feed kept on varying depending on the value of active input impedance Z_{aq}. If it is assumed that an identical voltage source is applied to each element, then the generator impedances $Z_{gq} = Z_q$ with $V_q = V$ for all q, where Z_g is the universal generator impedance. Thus, the expression for I_q can be re-written as:

$$I_q = \frac{V}{Z_{aq} + Z_g} \tag{3.8}$$

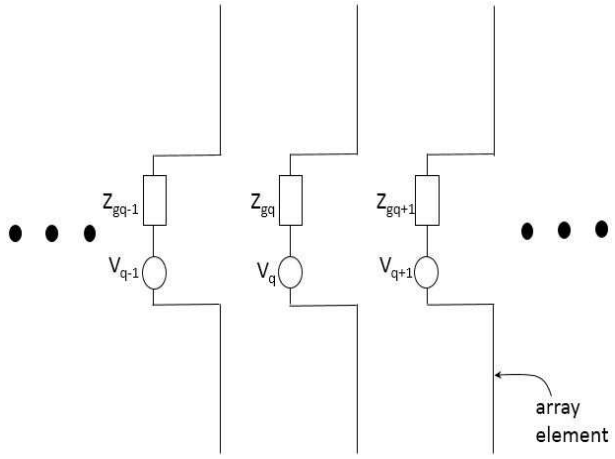

Figure 3.4: Thevenin Equivalent of Antenna Array

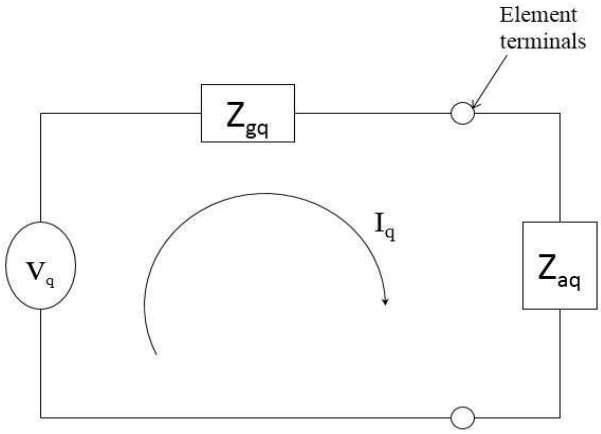

Figure 3.5: Thevenin Equivalent Circuit of One Element

Under conditions neglecting the effect of mutual coupling, the expression for voltage source V will be given as:

$$V = I * Z_g$$

where I is the current flowing through each antenna element in above condition.

Using above expression of V in 3.8, it can be finally reduced to a more general form in term of current I. Here, it can be noted that the expression for current excitation with mutual coupling effects solely depends on active input impedance as given under:

:

$$I_q = I * \frac{Z_g}{Z_{aq} + Z_g} \tag{3.9}$$

Let us consider the array factor expression for a general linear array without mutual coupling from equation 2.1 as:

$$AF(\theta,\phi) = \sum_{q=1}^{N} I_q * exp^{j[(n-1)kd\cos\theta+\beta]} \tag{3.10}$$

It is assumed that all the elements in the array are identical. Now, rewriting the above equation using 3.9, the Array Factor expression for linear array considering the effects of mutual coupling can be represented as:

$$AF_{mut}(\theta,\phi) = \sum_{q=1}^{N} I * \frac{Z_g}{Z_{aq}+Z_g} * exp^{j[(n-1)kd\cos\theta+\beta]} \tag{3.11}$$

In general,

$$AF_{mut}(\theta,\phi) = ImpedanceFactor * AF(\theta,\phi) \tag{3.12}$$

where,$\frac{Z_g}{Z_{aq}+Z_g}$ is the Impedance Factor due to mutual coupling.
Z_g is the generator impedance or self impedance of antenna element
Z_{aq} is the active input impedance or mutual-impedance of q_{th} antenna element

3.5 Simulation Results on Mutual Coupling Effects

Simulation of antenna arrays with mutual coupling effect is performed under the following assumptions:
a) Antenna array consists of isotropic radiator.
b) Each antenna element is oriented in z-direction.
c) Uniform Current Excitation source is applied to each element.
d) Element current distribution assumed to be uniform.
Referring to equation 3.6 and applying above mentioned assumptions, the mutual impedance for each element of the array is calculated. Using these results in equation 3.12, the array factor for each arrays with mutual coupling effect is formulated and the obtained radiation pattern is compared with the

radiation pattern without mutual coupling.

3.5.1 Case Study 1: Linear Array

The simulation result for linear array [7, 4] with 10 & 13 elements in z-direction is shown in fig.3.6 and 3.7. It can be observed that the shape of the radiation patterns remains same with the a small increment in its SLL. The main beam of both the radiation pattern also remains identical.

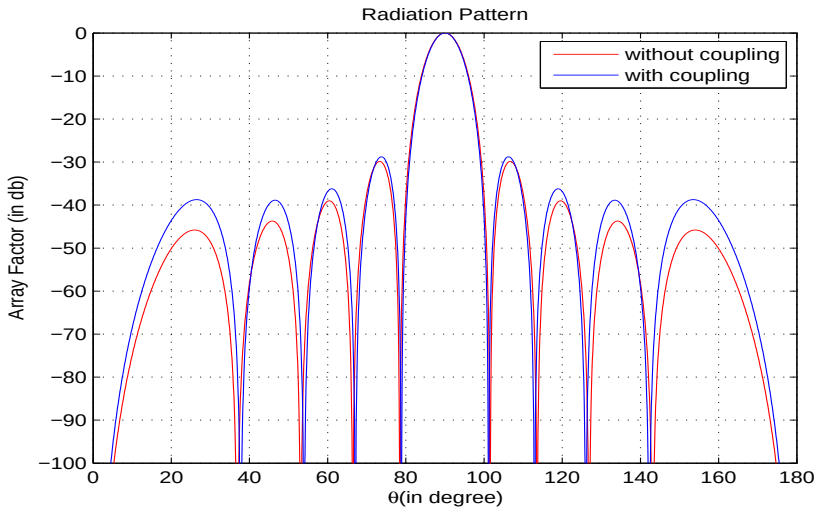

Figure 3.6: Radiation Pattern of 10 Elements Linear Array

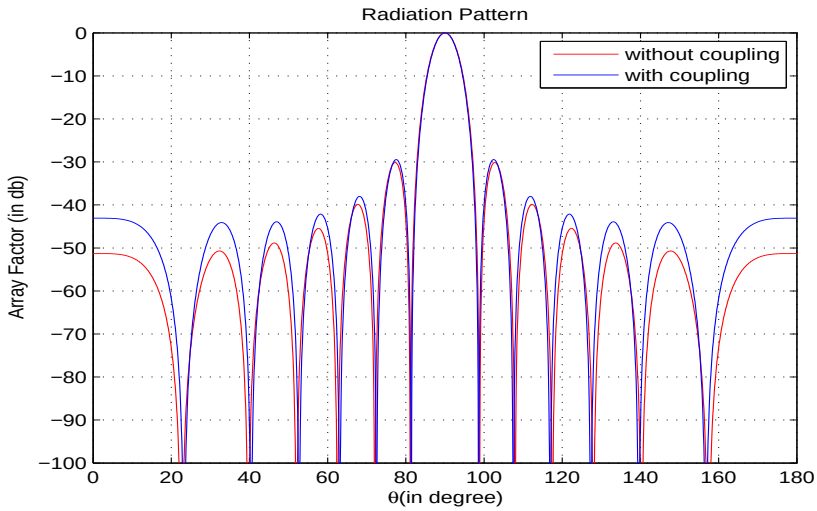

Figure 3.7: Radiation Pattern of 13 Elements Linear Array

3.5.2 Case Study 2: Planar Array

Planar array of size 4x4 & 5x5 is modelled in yz-plane and respective simulation result is shown in fig. 3.8 and 3.9. In these results, the radiation pattern along with its magnitude is also modified due to effect of mutual coupling thereby showing a tremendous impact of mutual coupling on planar arrays.

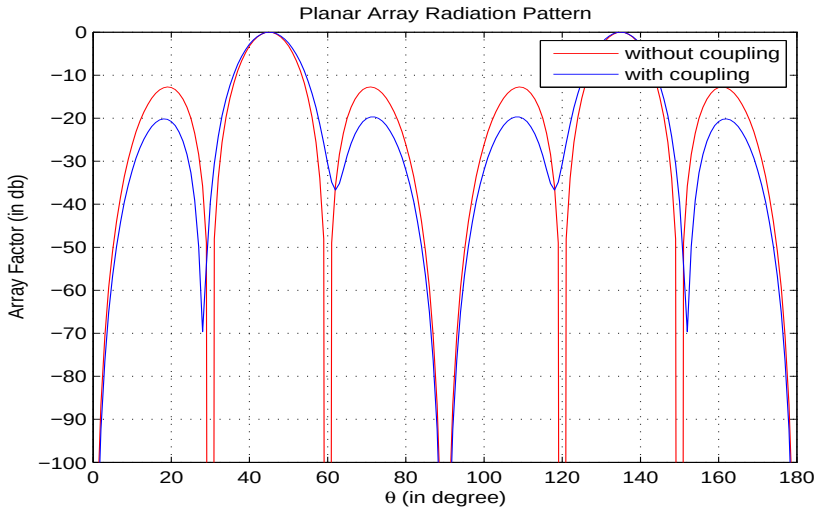

Figure 3.8: Radiation Pattern of 4x4 Planar Array

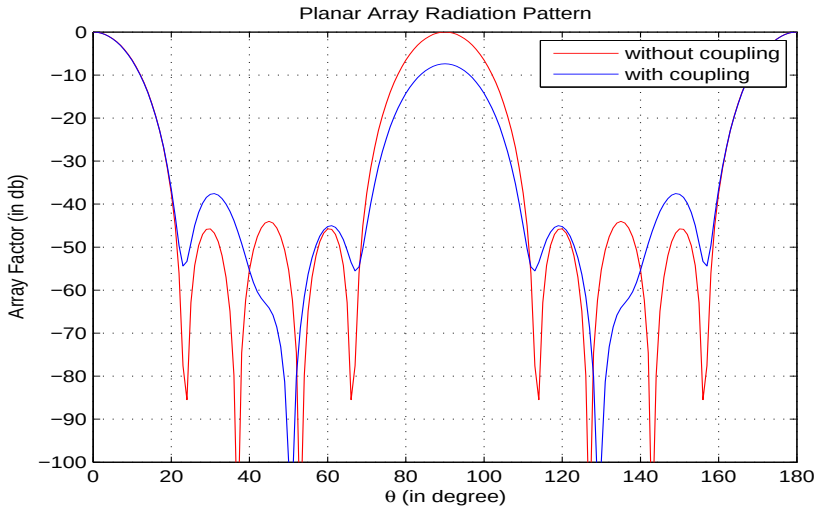

Figure 3.9: Radiation Pattern of 5x5 Planar Array

3.5.3 Case Study 3: Circular Array

The array factor for circular array [3] with 10 & 16 element is modelled in xz-plane and the simulated result is shown in fig.3.10 and 3.11. Here, the radiation pattern in both environment overlaps showing no any variation due to mutual coupling effects. This can be justified by the fact that each element in circular array sees the same environment with respect to other elements, and hence no any pattern variation is observed.

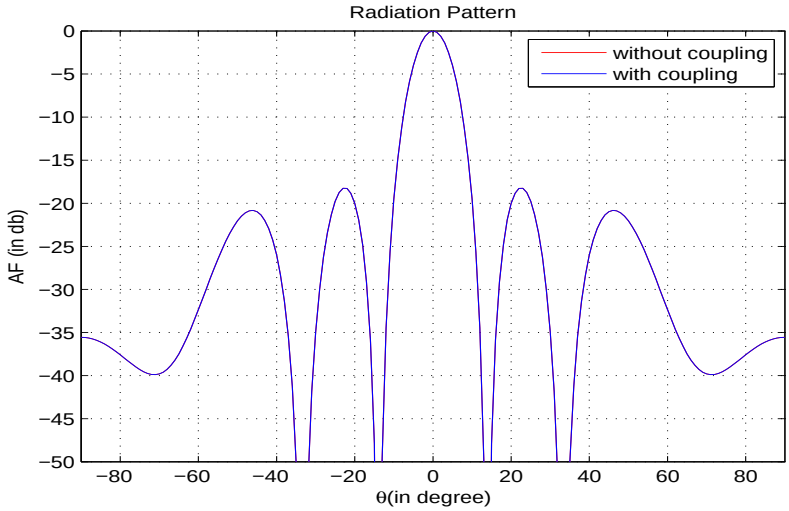

Figure 3.10: Radiation Pattern of 10 Elements Circular Array

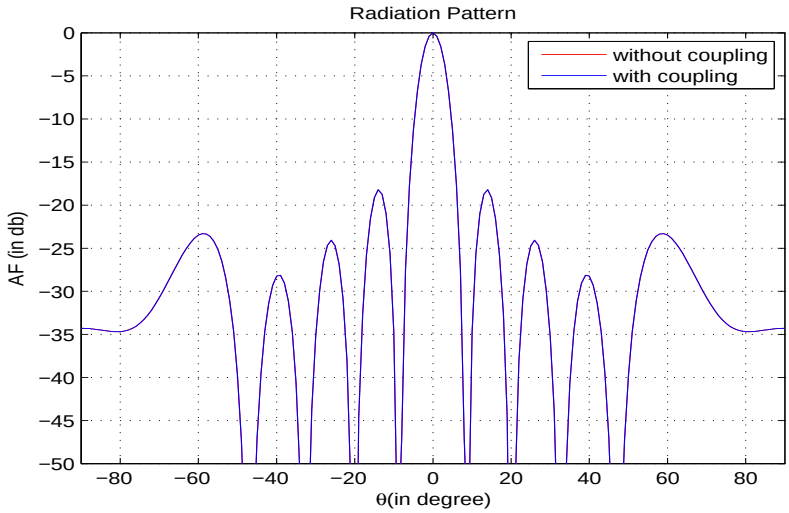

Figure 3.11: Radiation Pattern of 10 Elements Circular Array

3.5.4 Case Study 4: Spherical Array

Array factor of Spherical array with 54 and 106 elements under non-uniform element distribution is modelled and its radiation pattern is shown in fig.3.12 and 3.13. As seen in the results, it can be concluded that there is a very slight variation in radiation patterns due to almost similar environment seen by each element of the array. There is an uneven variation in SLL, which is lower for 54 elements array and gives a higher value for 106 elements array.

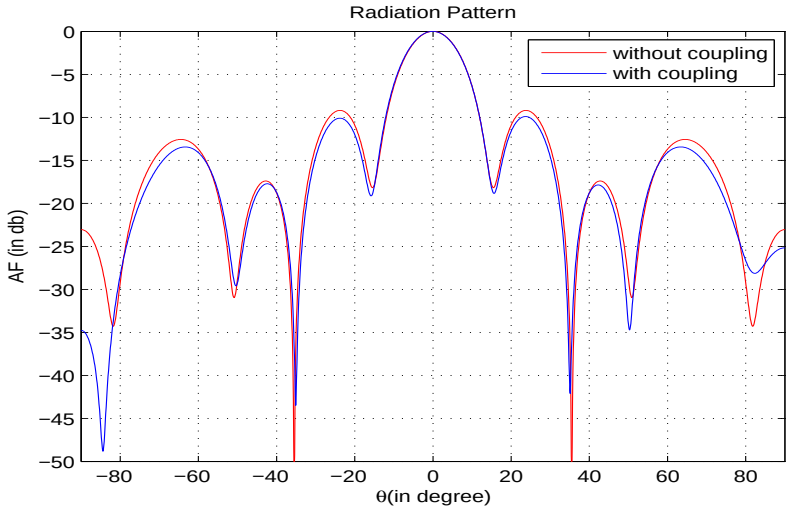

Figure 3.12: Radiation Pattern of 54 Elements Spherical Array

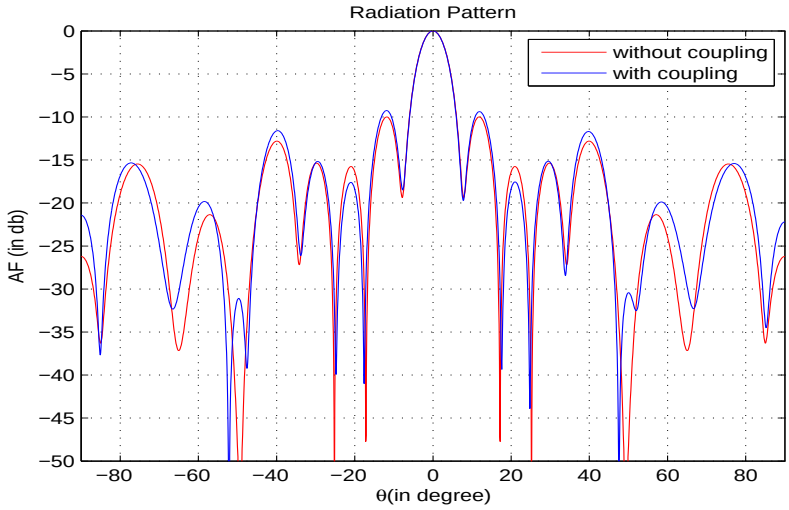

Figure 3.13: Radiation Pattern of 106 Elements Spherical Array

Chapter 4

Co-secant Square Shaped Pattern

In modern technology, shaped-beams are widely used in satellite and radar based applications. Cosecant-squared pattern(CSP) is one such pattern which is generally employed for long-range systems requiring higher gain near the horizon with low gain at higher elevation angles. During detection of an aircraft flying in space, it will be observed at a closer range at higher elevation angles, so use of such pattern significantly limits the power available to aircraft at higher elevation angles thereby providing a uniform signal strength to the aircraft throughout its journey. Thus, the cosecant squared pattern distribution [8] as shown in fig. 4.1 is a means of achieving a uniform signal strength at the input of the receiver of target when it is moving at a constant altitude.

4.1 Mathematical Justification of Cosecant-Squared Pattern

Consider an aircraft is flying at a constant height 'H' in an Air Surveillance radar System as shown in fig. 4.2. As it can be clearly observed that as the aircraft is moving towards the radar system, its range 'R' keeps on decreasing with an increase in its elevation angle 'θ'. Thus, due to this continuous variation in the range of aircraft, the echo power received by radar receiver keeps on changing. Thus, in order to receive uniform echo power by the receiver, the radiation shape needs to be modified to Cosecant-squared shape.

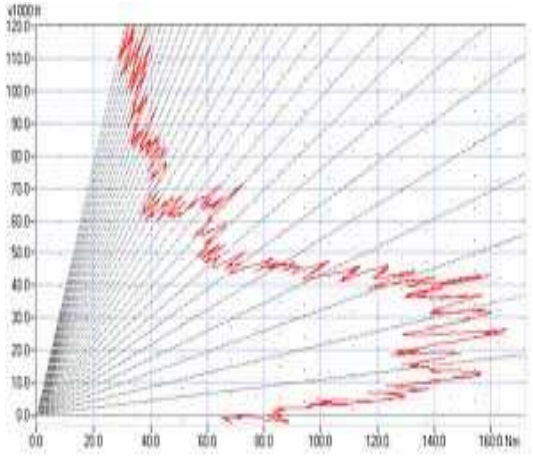

(a) A Practical Cosecant-Squared pattern Reference:radartutorial.eu

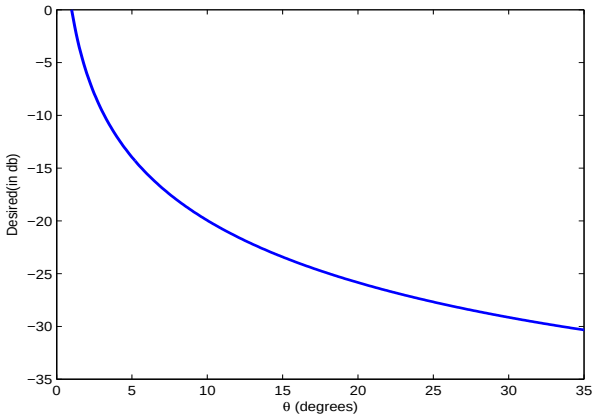

(b) Simulated Cosecant-Squared pattern

Figure 4.1: Cosecant-Squared Radiation Pattern

It can be justified from the derivation as below:

Referring to fig. 4.2, the range 'R' can be given as:

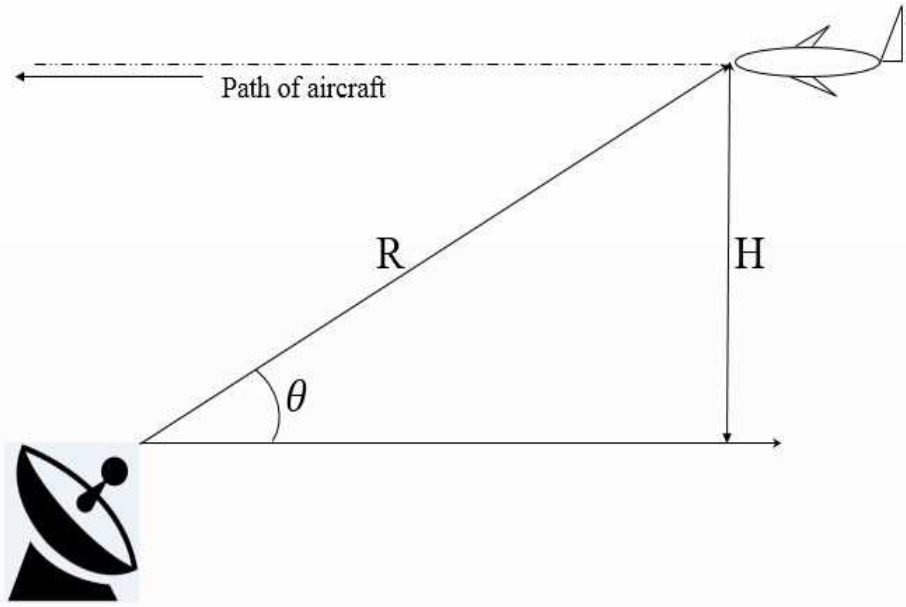

Figure 4.2: Air-Surveillance Radar System

$$R = \frac{H}{sin(\theta)} = H * cosec(\theta) \tag{4.1}$$

By Radar Range equation,the echo received by radar will be,

$$P_r \sim \frac{G^2}{R^4} \tag{4.2}$$

To receive uniform echo power by the radar receiver,

$$P_r = constant$$

Using above condition,equation (4.2) can be re-written as,

$$G^2 \sim R^4 \tag{4.3}$$

which will be further reduced to,

$$G \sim R^2 \tag{4.4}$$

Now using equation (4.1) in equ (4.4) we get,

$$G = (cosec(\theta))^2 \tag{4.5}$$

4.2 Optimization Algorithms

The above discussed cosecant-squared pattern is one specific pattern and has to be generated with various antenna arrays. To generate this pattern, we requires some definite combination of radiation pattern controlling parameters for array like excitation amplitude, phase, inter-element spacing etc so that the newly generated radiation pattern tends to approximate the desired radiation pattern. In present scenario, it is observed that many such problem statement requires efficient use of optimization algorithms [11] to reach the desired solutions under various constraints. Nowadays, stochastic-based optimization algorithms has become ineffective in several research areas. Due to this, Evolutionary algorithms and Swarm-based optimization due to their global behaviour and less number of controlling parameters are getting more importance. Here, DE and SSO algorithms are discussed in details and are applied to achieve the objective of this thesis.

4.2.1 Differential Evolution Algorithm

Differential Evolution(DE) algorithm, proposed by Price and Storn in 1996, is a stochastic population-based evolutionary algorithm [13] for optimizing multi-dimensional space variables. In present scenario, there are so many problems whose objective function are non-linear, noisy, flat and multi-dimensional having more than one local minima and other constraints. Such problems are difficult to solve analytically, hence DE based technique can be well utilized to find an approximate result for such problems [14]. Moreover, compared to other algorithms DE is more simpler and straightforward to implement with very few control parameters (F, CR and N). It is extremely capable in providing multiple solutions in a single run with lower value of space complexity. However, the convergence rate of DE algorithm is quite higher in comparison to other class of algorithms [13]. This class of evolutionary algorithms follows four basic steps [12, 20] as Initialization, Mutation, Recombination and Selection for its operation.

1. Initialization: To optimize a function with D real parameters, we have to select a population of size N (at least of size 4)with the parameter vector 'x' given as:

$$x_i, G = [x_{1,i,G}, x_{2,i,G}, \ \ldots\ldots\ x_{D,i,G}]$$

where, i = 1, 2, . . . , N

G is the generation number

The vector x is selected randomly from its bounded range $[x_j^L, x_j^U]$.

where, x_j^L is lower limit,

x_j^U is upper limit

After initialisation of every vector of the population, its corresponding fitness value is computed and best of these is stored for future reference.

2. Mutation: Now for each given parameter $x_{i,G}$, we will select three random vectors $x_{r1,G}$,$x_{r2,G}$ and $x_{r3,G}$ with distinct indices i, r_1, r_2 and r_3. Apply

mutation on it using equation as below:

$$v_{i,G+1} = x_{r1,G} + F(x_{r2,G} \sim x_{r3,G})$$

where, F is the mutation factor, such that F∈[0,2]

$v_{i,G+1}$ is called as donar vector

3. Recombination: Now recombination uses successful solutions obtained from the previous generation and generates a new trial vector from the elements of the previous target vector $x_{i,G}$ and the elements of the newly created donar vector $v_{i,G+1}$ based on the following relation:

$$u_{j,i,G+1} = \begin{cases} v_{j,i,G+1}, & \text{if } rand_{j,i} \leq \text{CR or } j = I_{rand} \\ x_{j,i,G}, & \text{if } rand_{j,i} > \text{CR and } j \neq I_{rand} \end{cases}$$

where,i = 1, 2, . . . , N ;

j = 1, 2, . . . , D

I_{rand} is a random integer[1,2,.....D] such that, $v_{i,G+1} \neq x_{j,i,G}$

4. Selection: Finally, selection for next generation vector is done by comparing fitness value due to trial vector $v_{i,G+1}$ and target vector $x_{i,G}$ using criteria

$$x_{i,G+1} = \begin{cases} x_{i,G+1}, & \text{if } f(u_{1,G+1}) \leq f(x_{1,G}) \\ x_{i,G}, & \text{otherwise} \end{cases}$$

Now, the process of Mutation, Recombination and Selection is repeated till some stopping criterion as defined in the algorithm is reached.

The concept of DE algorithm process is presented with the flowchart [21] shown by fig. 4.3 as:

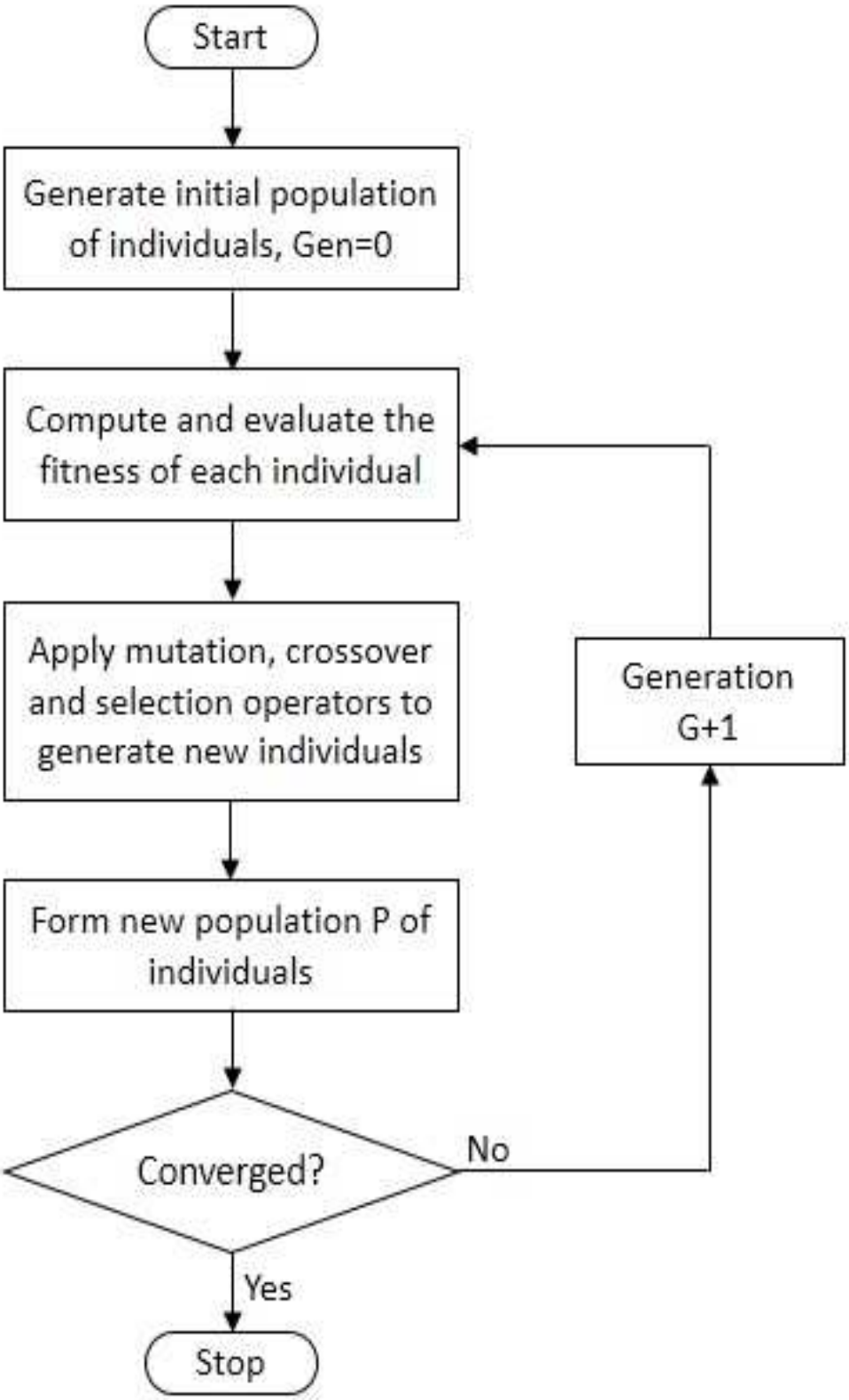

Figure 4.3: Flowchart of DE optimization Process

Validation of DE with the Published Work

Referred to [17] of Symmetric Linear array with 24 elements with uniform spacing of 0.5λ to minimise the SLL value. It is observed from the paper that GA optimization algorithm gives a SLL of -34.5dB with excitation amplitude optimization. Applying same constraints as mentioned in [17] with DE algorithm having parameters as mentioned in Table4.1, it is observed from fig. 4.4 that SLL reaches a value of -38.42dB for amplitude variation as indicated in Table 4.2.

Table 4.1: Parameters Used for DE Validation

S No.	Parameters	Value
1	Number of Elements	24
2	Inter-element Spacing	0.5λ
3	Population Size	50
4	Iterations	1000
5	θ_{MLL}	(76,104)
6	θ_{SLL}	[0,76]&[104,180]
7	F CR VTR	0.8 0.3 0

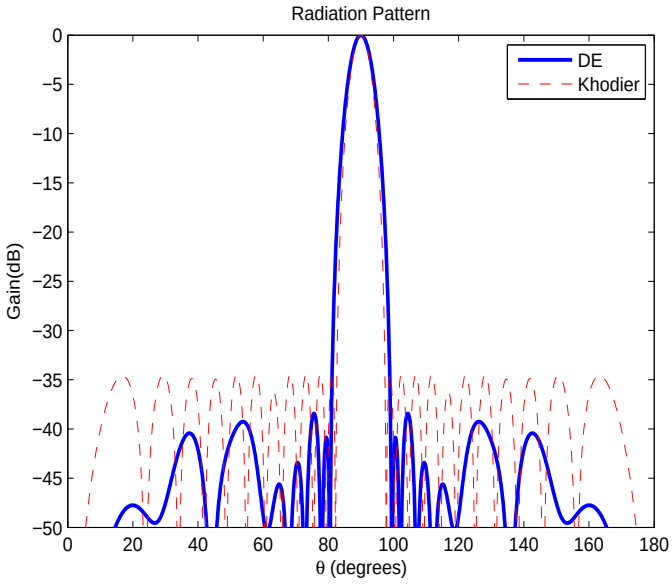

(a) Radiation Pattern Comparision

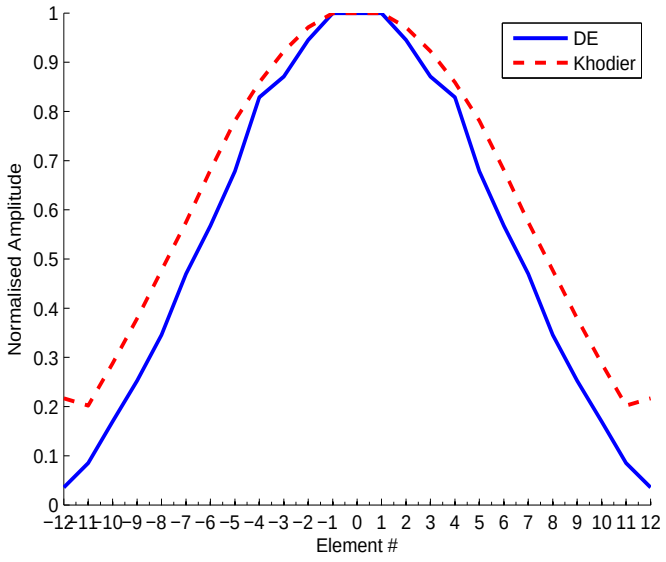

(b) Normalized amplitude distribution $|I_n|$ of array elements

Figure 4.4: Comparison Between DE and PSO(Khodier) for N=24 Symmetric Linear Array

Table 4.2: Performance Comparison between DE and PSO (Khodier)

Algorithms	Normalised Amplitude(I_n)	SLL(in dB)
PSO(Khodier)	1.0000,0.9712,0.9226,0.8591,0.7812,0.6807 0.5751,0.4768,0.3793,0.2878,0.2020,2167	-34.5
DE	1.0000,0.9454,0.8709,0.8288,0.6783,0.5676 0.4699,0.3457,0.2525,0.1695,0.0852,0.0355	-38.42

4.2.2 Simplified Swarm Optimization Algorithm

Simplified Swarm optimization(SSO) is an emerging met-heuristic algorithm which searches for best values with the help of population (swarm) of individuals (particles) which gets updated to better values with each iterations. It is derived from Particle Swarm optimization(PSO), as a simplified version of PSO technique It is designed to remove the premature convergence of PSO in high-dimensional multi-modal problems [15, 16]. Thus, SSO is able to improve the convergence speed with increase in number of iterations. SSO starts with some size of swarm population having random position of particles, maximum number of generations and three controlling parameters C_w, C_p & C_g depending on the application. In every generation, the particle's position value in each dimension keeps on updating to some new pbest value or gbest value or some random value according to following criteria as under [15]:

$$x_{id}^{t} = \begin{cases} x_i^{t-1}, & \text{if rand}() \in [0, C_w) \\ p_i^{t-1}, & \text{if rand}() \in [C_w, C_p) \\ g_i^{t-1}, & \text{if rand}() \in [C_p, C_g) \\ x, & \text{if rand}() \in [C_g, 1) \end{cases}$$

here, i=1,2,.....m; where m is size of swarm

$$X_i = (x_{i1}, x_{i1}, \ ..... \ x_{iD})$$

where, x_{iD} is the position value of the i_{th} particle for D_{th} space dimension. C_w, C_p & C_g are three constant positive parameters such that

$$C_w \ < \ C_p \ < \ C_g$$

$P_i = (p_{i1}, p_{i1}, \ ..... \ p_{iD})$ denotes the best solution achieved by each individuals (pbest),
$G_i = (g_{i1}, g_{i1}, \ ..... \ g_{iD})$ denotes the best solution achieved so far by the whole swarms (gbest),
x represents the new value for the particle in every dimension which are randomly generated from random function 'rand()'; where, the random number can be taken between 0 and 1.
The SSO algorithm is explained in detail by the flowchart fig. 4.5 shown below:

Validation of SSO

Referred to AF of circular array [9] of 30 isotropic elements with inter-element spacing of 0.5λ, optimization based on SSO algorithm has been applied under mentioned constraints and compared with GA results to show the superiority of SSO over GA. The various parameters considered for this comparison [9] are shown in Table 4.3. It is observed from the simulated result fig. 4.6 & Table 4.4 that there is a drastic reduction in side lobe level which reduces from -10.88dB with Genetic algorithm used in [9] to a value of -13.11dB with the proposed SSO algorithm. Moreover, no ripples are observed with proposed scheme showing an upper hand of the proposed scheme.

Table 4.3: Parameters Used for SSO Validation

S No.	Parameters	Value
1	Number of Elements	30
2	Inter-element Spacing	0.5λ
3	Population Size	50
4	Iterations	500
5	θ_{CSC}	(0,30)
6	θ_{SLL}	(-90,0)&(30,90)
7	C_g C_p C_w	[0.45,0.65] (0.65,0.85] (0.85,0.95]

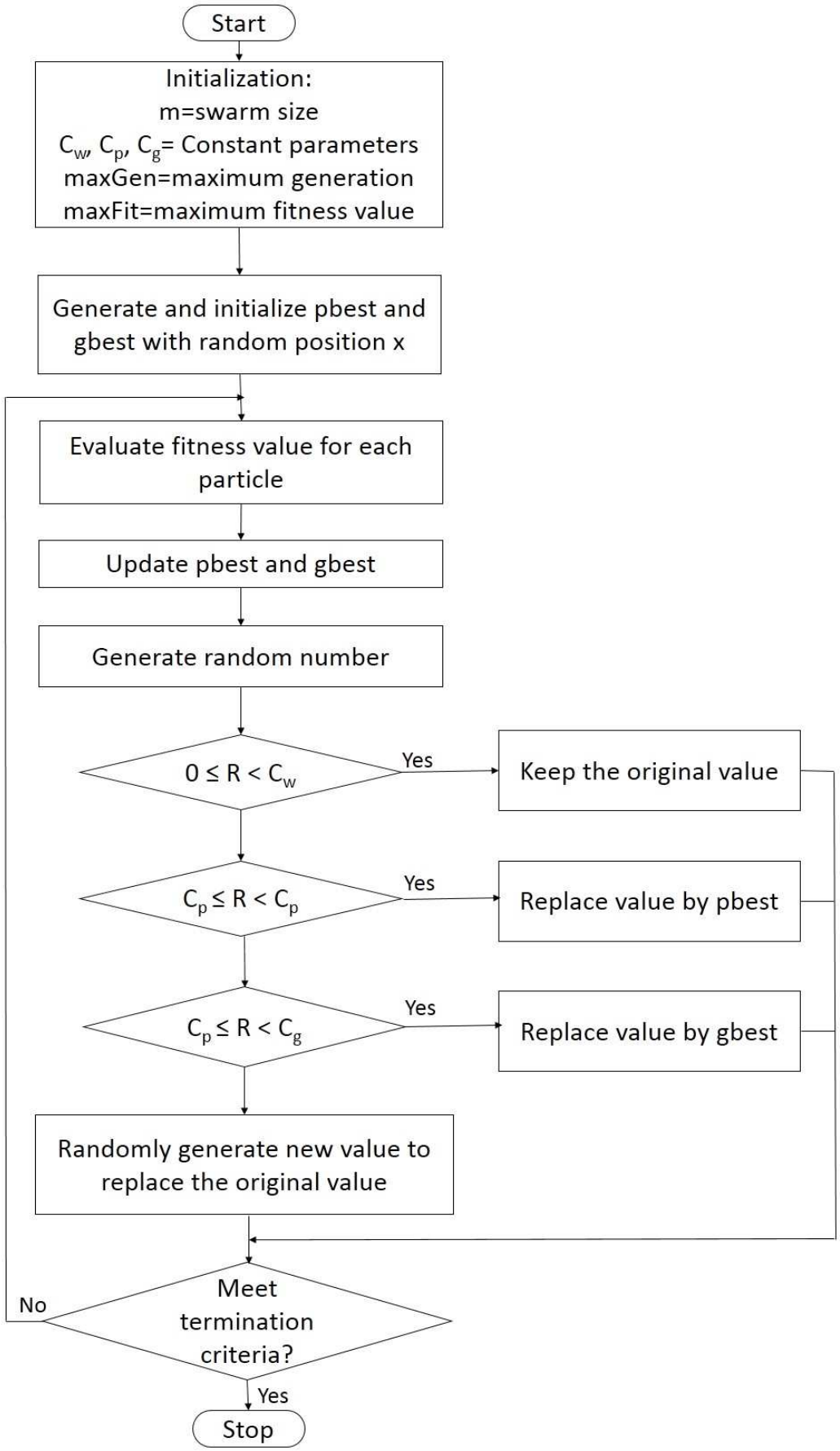

Figure 4.5: Flowchart of SSO Algorithm

Table 4.4: Desired & Obtained Results

Parameter	Desired	GA	SSO
SLL(in dB)	-15	-10.88	-13.11

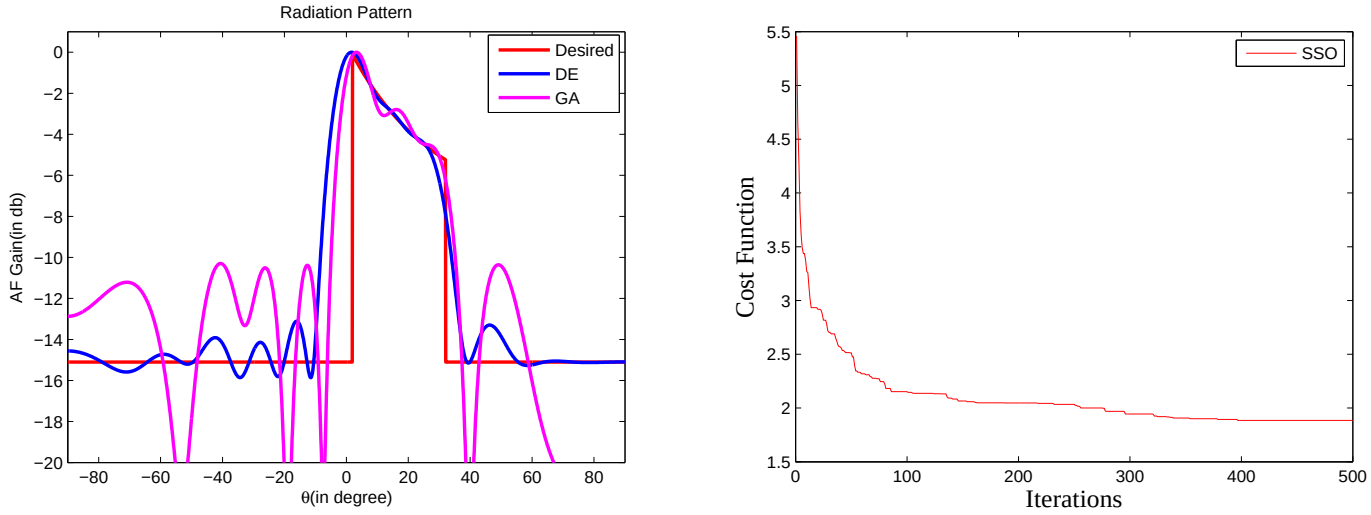

(a) Radiation Pattern

(b) SSO Cost Function

Figure 4.6: Comparison Result between SSO & GA for N=30 Circular Array

4.3 Simulation Results for Cosecant-Squared Shaped Pattern

Applying basic Differential evolution(DE) and Simple Swarm optimization(SSO) algorithms on linear, circular and spherical array, cosecant-squared pattern is generated. The desired pattern used for linear & circular as shown in fig.4.7a is plotted against elevation angle θ and for spherical as shown in fig. 4.7b is plotted against azimuthal angle ϕ with two cosecant-squared curves of 35° each.

The calculation of ripple component in the obtained $cosec^2$ pattern is given by cumulative summation of the deviation Δ_{ripple} in cosecant curve from desired curve as :

$$\Delta_{ripple} = \Delta_{CSC} = \sum_{\theta \in [cscrange]} |AF(\theta, 90) - Desired(\theta, 90)| \qquad (4.6)$$

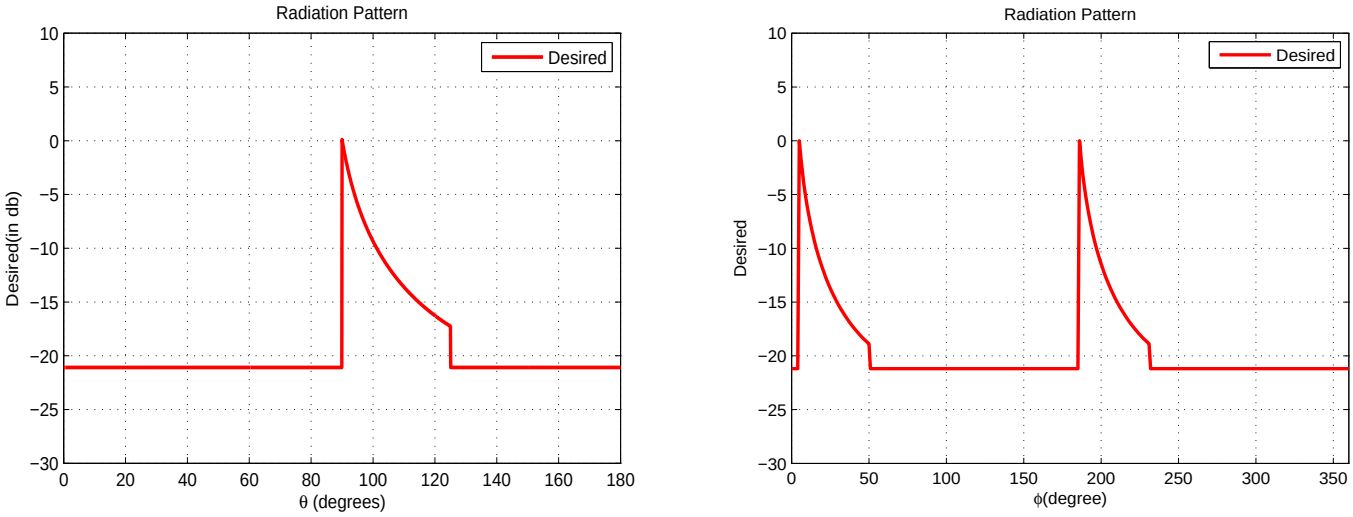

(a) Desired Pattern for Linear & Circular Array

(b) Desired Pattern for Spherical Array

Figure 4.7: Desired Cosecant-Squared Pattern for Linear, Circular & Spherical Array

4.3.1 Case Study 1: Linear Array

A linear array of 30 isotropic elements [8, 10] placed along y-axis with array factor as given in equation (4.7) is considered. Here, excitation amplitude($|I_n|$), phase(ϕ_n) as well as distance(d_n) are simultaneously optimized to generate the desired cosecant-squared pattern.

$$AF_{lin}(\theta, \phi) = \sum_{n=1}^{N} I_n * exp^{j[(n-1)kd_n \sin\theta]} \tag{4.7}$$

where, $I_n = |I_n|e^{j\phi_n}$ is the excitation coefficient for n_{th} element.
The fitness function used with the algorithms for generation of cosecant-squared pattern is given by equation (4.8) as:

$$f_{cost} = 0.65 * \Delta_{CSC} + 0.2 * \Delta_{SLL} + 0.15 * \Delta \tag{4.8}$$

where, $\Delta = \sum_{\theta\in[-90,90]} |AF(\theta, 90) - Desired(\theta, 90)|$
$\Delta_{CSC} = \sum_{\theta\in[0,35]} |AF(\theta, 90) - Desired(\theta, 90)|$
$\Delta_{SLL} = \sum_{\theta\in[-90,0]\&[30,90]} |AF(\theta, 90) - Desired(\theta, 90)|$

It is observed from fig. 4.8 & 4.9 that in each case the main beam curve consist of significant amount of ripple component with higher value of SLL.

It can be clearly concluded that, SSO performs better in terms of both convergence rate and SLL constraint against DE based optimization.

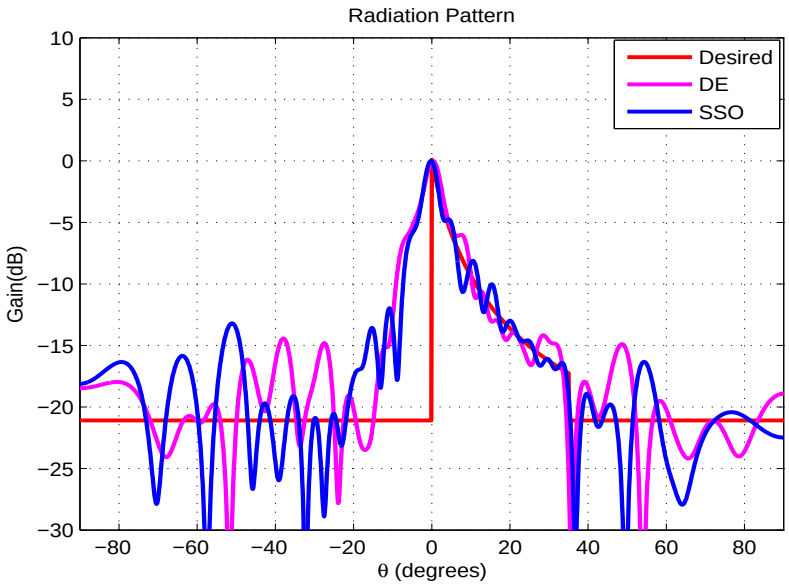

(a) Radiation Pattern for N=30 Elements

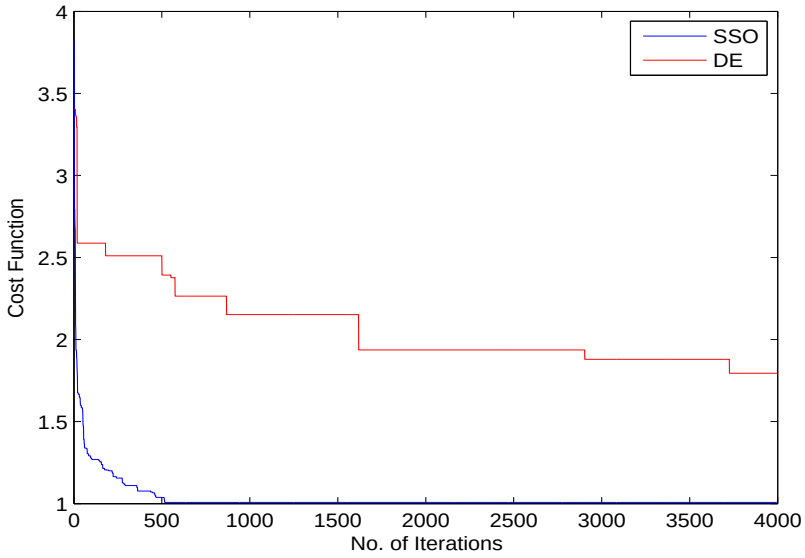

(b) Cost Function for N=30 Elements

Figure 4.8: Linear Array Simulation Result with DE and SSO

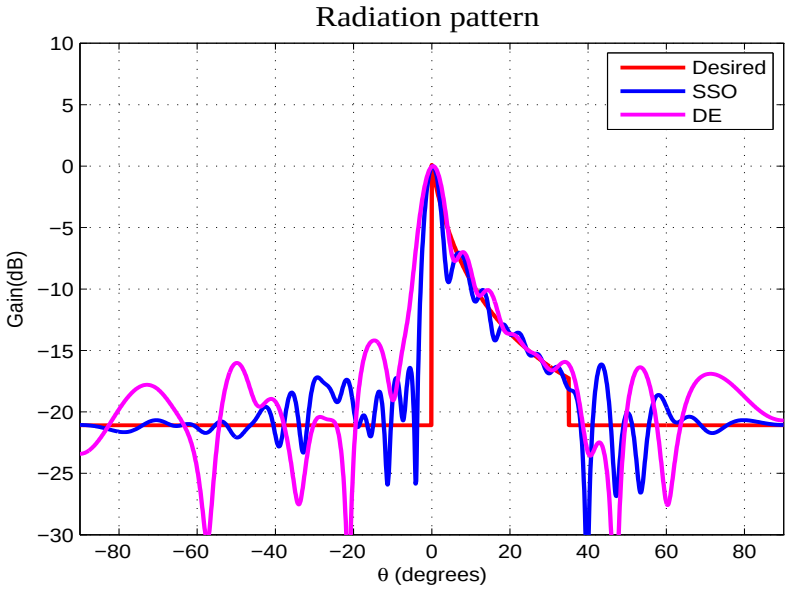

(a) Radiation Pattern for N=30 Elements

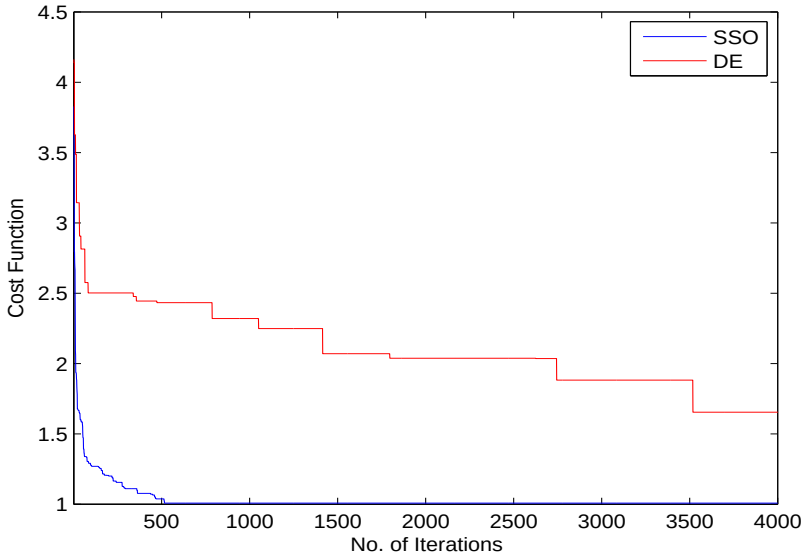

(b) Cost Function for N=30 Elements

Figure 4.9: Linear Array Simulation Result with DE and SSO

Table 4.5: Performance Comparison for N=30 & N=40 Elements Linear Array

No. of Elements	Side Lobe Level(in dB)			Deviation 'Δ_{ripple}'(in dB)		
	Desired	DE	SSO	Desired	DE	SSO
N=30	-21.09	-14.43	-13.20	0.00	36.67	23.17
N=40	-21.09	-14.18	-16.14	0.00	20.60	19.11

4.3.2 Case Study 2: Circular Array

A circular array [9] of 30 & 40 isotropic elements placed at equal spacing in xy-plane is considered whose array factor is given by equation (4.9). Here, unlike the case of linear array only amplitude($|I_n|$) & phase(ϕ_n) of the array factor is optimized.

$$AF_{cir}(\theta,\phi) = \sum_{m=1}^{M} I_m * exp^{j[ka\sin\theta\cos(\phi-\phi_m)]} \tag{4.9}$$

where, $I_m = |I_m|e^{j\alpha_m}$ is the excitation coefficient for m_{th} element.
$|I_m|$ is the normalised amplitude and α_m is the phase of the excitation coefficient for m_{th} element.
The fitness function taken for the desired pattern in circular array is given by equation (4.10) as

$$f_{cost} = 0.65 * \Delta_{CSC} + 0.25 * \Delta_{SLL} + 0.10 * \Delta \tag{4.10}$$

where, $\Delta = \sum_{\theta\in[-90,90]} |AF(\theta,90) - Desired(\theta,90)|$
$\Delta_{CSC} = \sum_{\theta\in[0,35]} |AF(\theta,90) - Desired(\theta,90)|$
$\Delta_{SLL} = \sum_{\theta\in[-90,0]\&[30,90]} |AF(\theta,90) - Desired(\theta,90)|$
It can be observed that as compared to linear array fig. 4.8a & 4.11a, pattern of circular array fig. 4.10a & 4.11ahas more smoother curve in the main beam. Also, with increase in the number of elements from N=30 to N=40, main beam width decreases showing a closer pattern to the required desired pattern. Further, comparing the cost function fig. 4.10b & 4.11b for N=30 & N=40 also shows an improvement in convergence rate with SSO technique against DE.

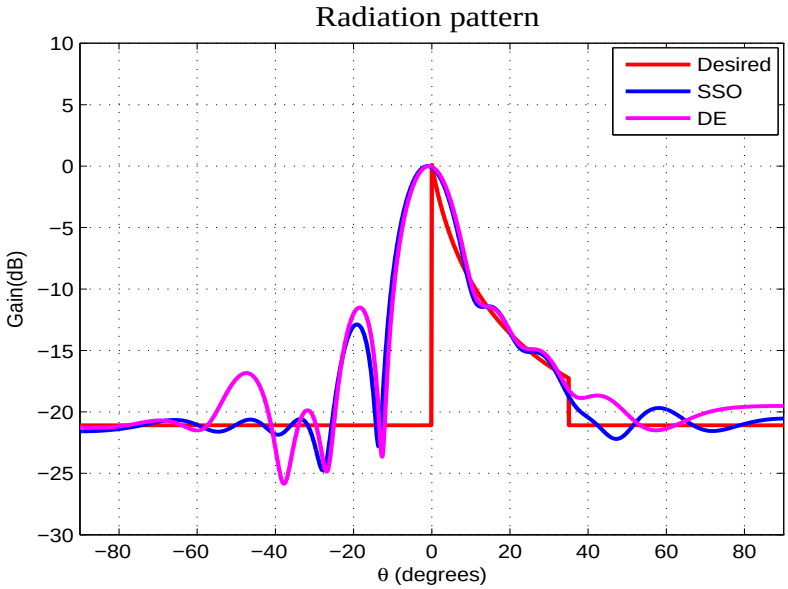

(a) Radiation Pattern for N=30 Elements

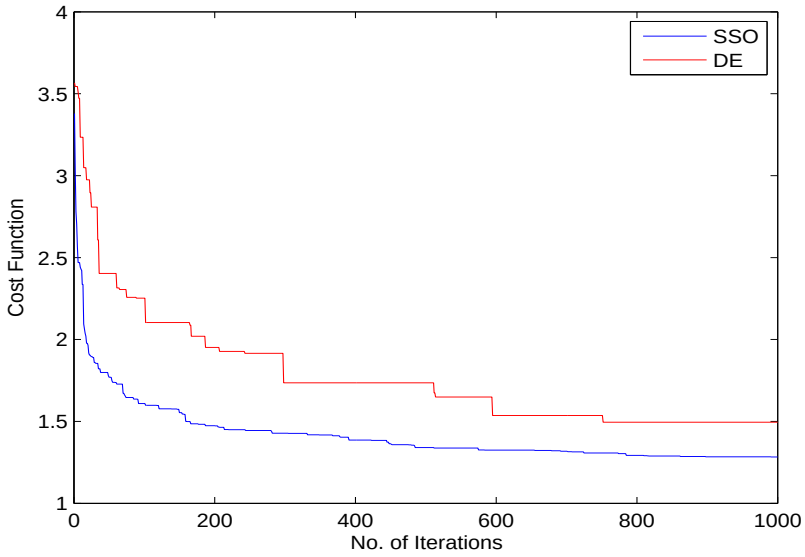

(b) Cost Function for N=30 Elements

Figure 4.10: Circular Array Simulation Result with DE and SSO

Table 4.6: Performance Comparison for N=30 & N=40 Elements Circular Array

No. of Elements	Side Lobe Level(in dB)			Deviation 'Δ_{ripple}'(in dB)		
	Desired	DE	SSO	Desired	DE	SSO
N=30	-21.09	-11.51	-12.88	0.00	28.91	27.81
N=40	-21.09	-13.68	-15.32	0.00	22.08	24.79

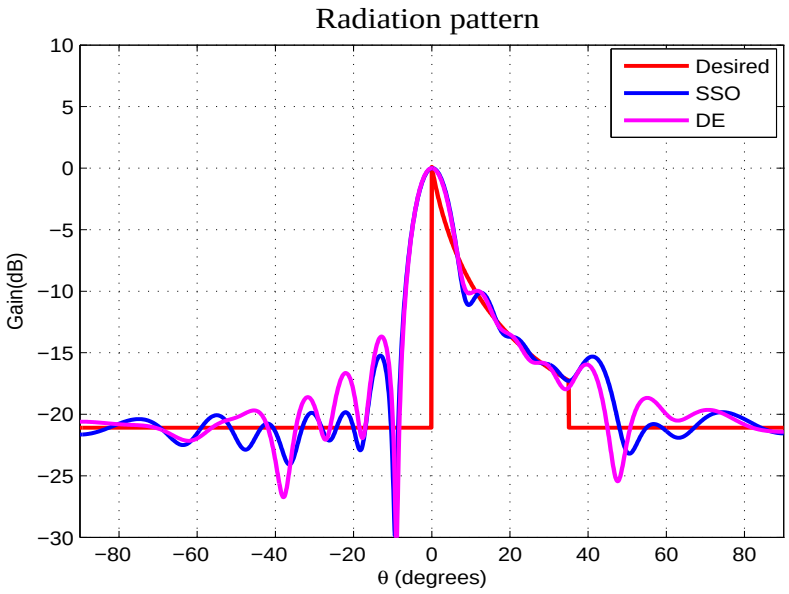

(a) Radiation Pattern for N=40 Elements

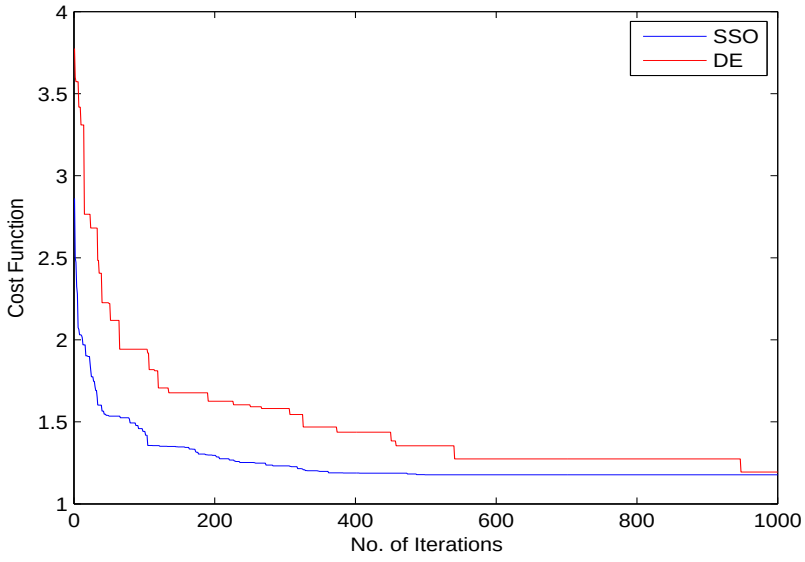

(b) Cost Function for N=40 Elements

Figure 4.11: Circular Array Simulation Result with DE and SSO

4.3.3 Case Study 3: Spherical Array

An array factor of spherical array with 54 & 106 isotropic elements placed such that 20 & 40 elements are in main circular array, 16 & 32 elements are in sub-circular arrays and single element is at the top and the bottom as in equation (4.11) with I_{mn} optimization is considered:

$$AF_{sph}(\theta,\phi) = \sum_{n=-1}^{1}\sum_{m=1}^{M_n} I_{mn} exp^{(jka_n sin(\theta)cos(\phi-\phi_{mn})+j\psi_m)+(jkd_n cos(\theta))} + exp^{(jka_0\cos\theta)} + exp^{(-jka_0\cos\theta)} \quad (4.11)$$

$I_{mn} = |Imn|e^{j\psi_m}$ is the current excitation for m_{th} antenna element of n_{th} circular array,

$|I_{mn}|$ is the normalised amplitude and ψ_m is the phase of excitation,

ϕ_{mn} is the azimuth position of m_{th} antenna element on n_{th} circular array,

a_n is the radius for n_{th} circle of spherical array,

a_0 is the radius of spherical array,

d_n is the distance of n_{th} circular array from reference circular array at the origin,

The fitness function used for spherical array is given by equation as:

$$f_{cost} = 0.75 * \Delta_{CSC} + 0.25 * \Delta_{SLL} + 0.00 * \Delta \quad (4.12)$$

where, $\Delta = \sum_{\phi\in[0,360]} |AF(90,\phi) - Desired(90,\phi)|$

$\Delta_{CSC} = \sum_{\phi\in[0,35]\&[158,218]} |AF(90,\phi) - Desired(90,\phi)|$

$\Delta_{SLL} = \sum_{\phi\in[36,180]\&[216,360]} |AF(90,\phi) - Desired(90,\phi)|$

It can be observed from simulation results fig. 4.12a & 4.13a that radiation pattern for N=106 elements performs well as compared to N=54 elements spherical array. Further, the main beam and SLL in each case of spherical array significantly follows the desired main beam and the SLL level. Moreover, no any ripples are observed in the obtained cosecant-squared pattern. The cost function in fig. 4.12b & 4.13b clearly indicates that SSO converges much more rapidly as compared to convergence of DE.

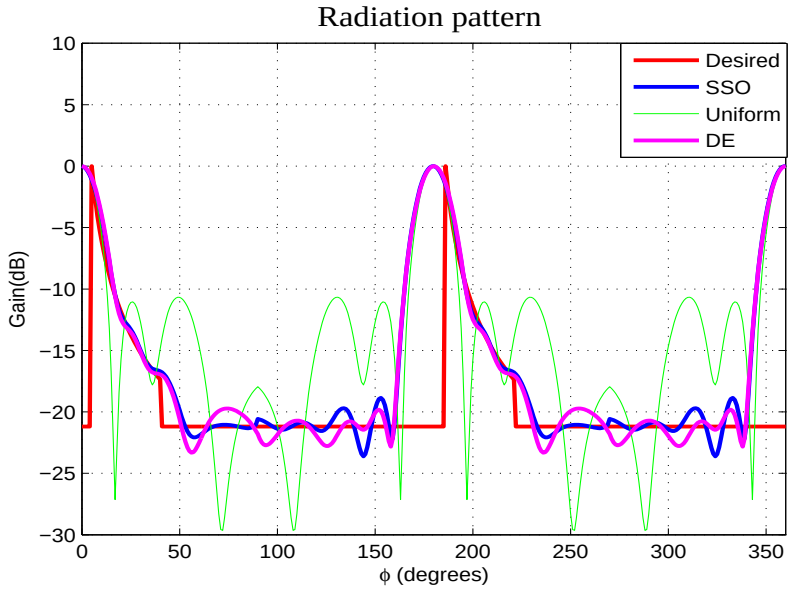

(a) Radiation Pattern for N=54 Elements

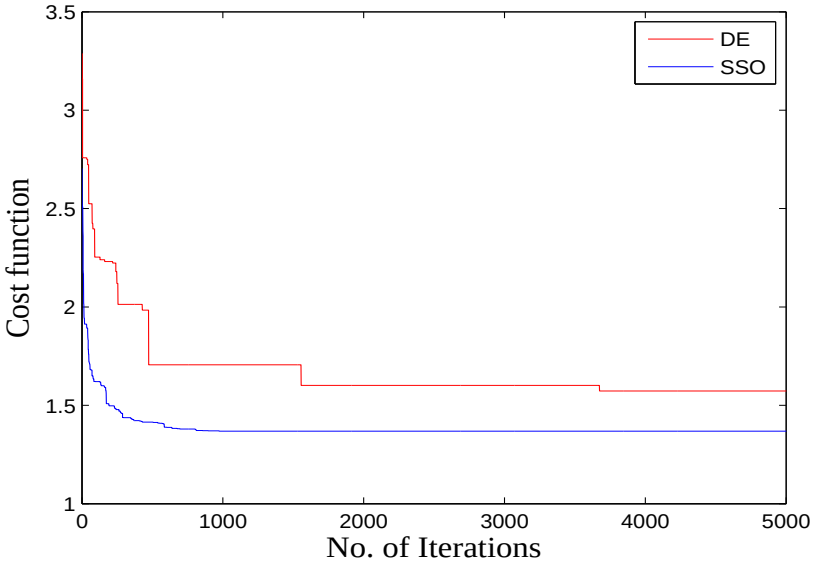

(b) Cost Function for N=54 Elements

Figure 4.12: Spherical Array Radiation Pattern with DE and SSO

Table 4.7: Performance Comparison for N=54 & N=106 Elements Spherical Array

No. of Elements	Side Lobe Level(in dB)			Deviation 'Δ_{ripple}'(in dB)		
	Desired	DE	SSO	Desired	DE	SSO
N=54	-21.19	-19.73	-18.86	0.00	18.94	10.88
N=106	-21.19	-16.80	-17.66	0.00	22.16	17.62

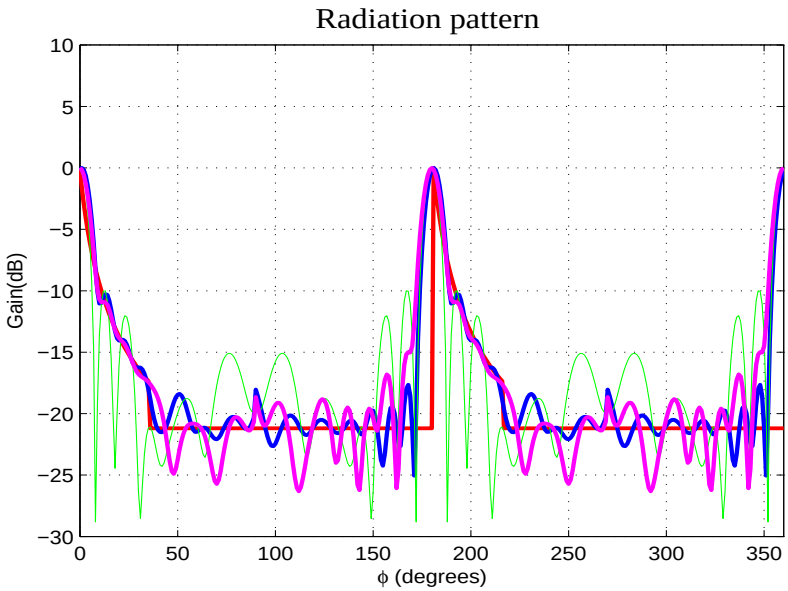

(a) Radiation Pattern for N=106 Elements

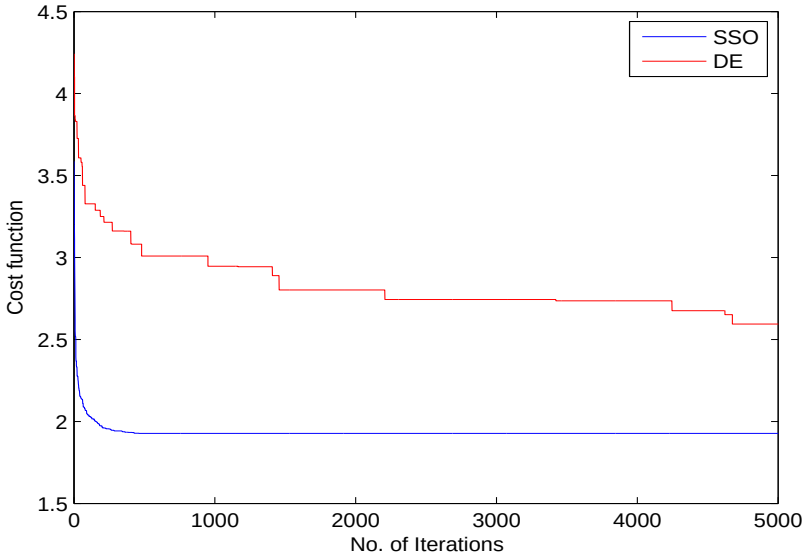

(b) Cost Function for N=106 Elements

Figure 4.13: Spherical Array Radiation Pattern with DE and SSO

Table 4.8: Performance Comparison for Antenna Arrays with DE & SSO

Array	Side Lobe Level(in dB)					Deviation 'Δ_{ripple}'(in dB)			
	Desired	Worst		Best		Worst		Best	
		DE	SSO	DE	SSO	DE	SSO	DE	SSO
Linear	-21.09	-14.43	-13.20	-14.18	-16.14	36.67	23.17	20.60	19.11
Circular	-21.09	-11.51	-12.88	-13.68	-15.32	28.91	27.81	22.08	24.79
Spherical	-21.09	-16.80	-17.66	-19.73	-18.86	18.94	10.88	22.16	17.62

4.4 Implementation in Graphical User Interface

Graphical User Interface is a programming interface that takes the advantages of computer graphics capabilities to make the program user-friendly. It makes the user free from learning command code language, thereby making easier for the users to use the application efficiently. A GUI of Spherical antenna array is framed in which number of elements, iterations, best runs, DE parameters(F & CR) and SSO parameters(C_g, C_p, C_w) are taken as inputs. Commanding buttons like 'DE', 'SSO' and 'Run All' are used to generate the outputs as Radiation Pattern, Fitness Plot and Optimised values(Ripple factor, Side lobe Level). Here, 'DE' & 'SSO' button will perform optimization with Differential algorithm and Simplified Swarm optimization respectively, while 'Run All' button will perform both optimization simultaneously and will show the better result of the two in terms of optimized value as output.

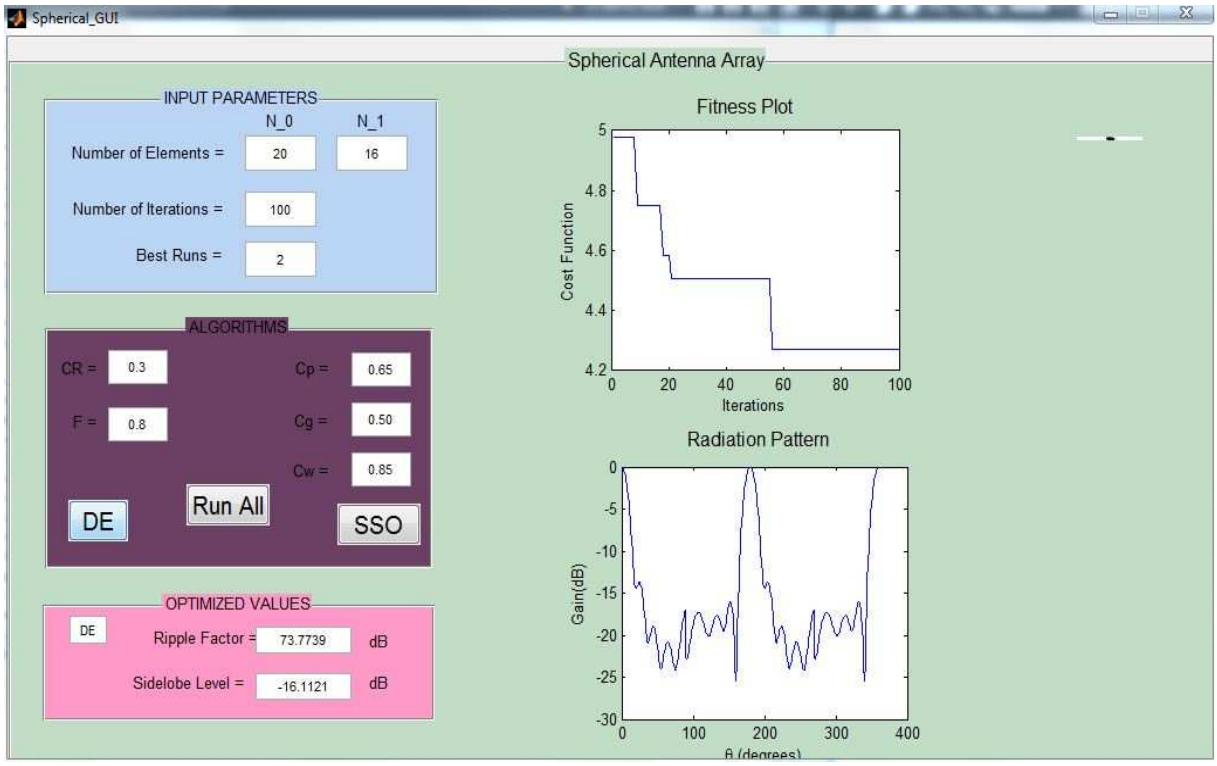

Figure 4.14: GUI Model of Spherical Antenna Array

Chapter 5

INDIA-SHAPED Radiation Pattern

In recent scenario of technological advancement, every country needs to have an access of its complete geographical region as well as its international boundary line for security purpose, meteorological informations and for many more such like requirements. So, it becomes necessary to have full communication access to each and every corner of the country with least amount of expenditure of resources. Thus, if a single antenna array system is utilized in such a way that it generates a radiation pattern which resembles with the geographical boundary of a country, then, a lots of energy and other resources involved in the existing communication system can be saved.

5.1 Problem Formulation

A desired pattern which resembles with the Indian geographical boundary line is created taking the central location of India as the reference position of antenna system used. Here, as the required boundary coverage varies in every direction fig. 5.1b, so an antenna system whose radiation pattern is approximately omni-directional in nature such as spherical, conical, hexagonal antenna array etc can be taken for the generation of desired pattern. The desired India-shaped Radiation pattern to be generated by the antenna system is shown in fig. 5.1 where fig. 5.1a shows the 2D plot in dB and fig.

5.1b gives the normalized polar plot. An error of maximum 0.02 in magnitude and 2° in angle may be present in the polar radiation pattern due to complexity in the Indian boundary-line. It can be observed that the desired polar plot pattern fig. 5.1b approximately resembles with the geographical international boundary-line of India.

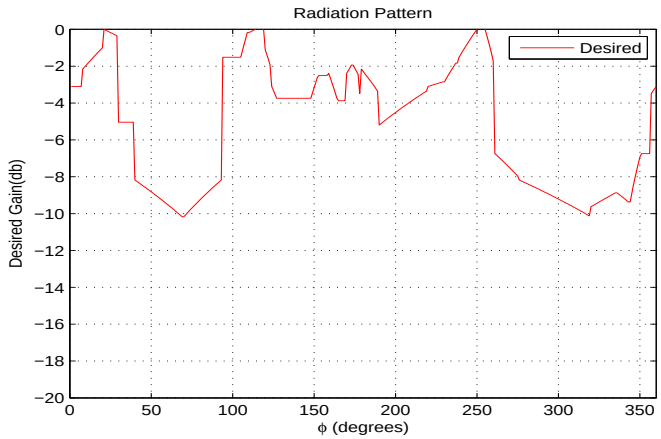

(a) Desired 2D Radiation Pattern

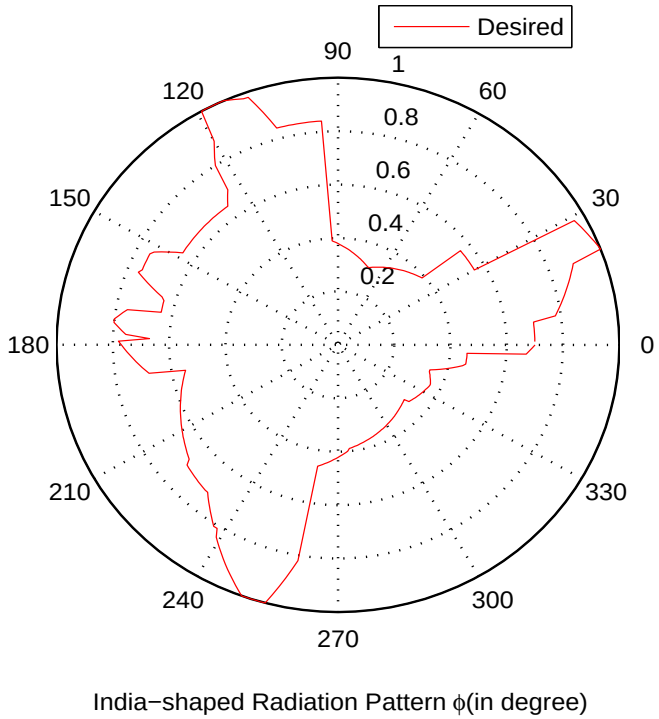

(b) Desired Polar Radiation Pattern

Figure 5.1: Desired India-Shaped Radiation Pattern

5.2 Simulation Results for India-Shaped Pattern

A spherical array with AF given by equation (4.11) of 54 isotropic antenna elements such that 20 elements in main circle, 16 elements in each sub-circles and single element at the top and bottom is taken for the generation of the desired pattern. As the desired radiation pattern has a 360° coverage, so the plot is taken against azimuth direction 'ϕ' with elevation angle as 90°. Here, both amplitude($|I_n|$) and phase(ϕ_n) of excitation coefficient is optimized using DE & SSO algorithms. The DE parameters are F, CR and VTR and values used for the process are F=0.8, CR=0.3, VTR=0 with population of size 50. Further, the parameters used with SSO technique with the population of size 100 are C_g, C_p & C_w and are defined by the equation given below as:

$$C_g = 0.45 + rand * (0.65 - 0.45)$$

$$C_p = 0.651 + rand * (0.85 - 0.651)$$

$$C_w = 0.851 + rand * (0.95 - 0.851)$$

The objective function used with the spherical array to get the optimised India-shaped radiation pattern is given by equation (5.1) as:

$$f_{obj} = 0.60 * \Delta + 0.25 * \Delta_1 + 0.07 * \Delta_2 + 0.08 * \Delta_3 \tag{5.1}$$

where, $\Delta = \sum_{\phi\in[0,360]} |AF(90,\phi) - Desired(90,\phi)|$
$\Delta_1 = \sum_{\phi\in[145,265]} |AF(90,\phi) - Desired(90,\phi)|$
$\Delta_2 = \sum_{\phi\in[8,28]} |AF(90,\phi) - Desired(90,\phi)|$
$\Delta_3 = \sum_{\phi\in[100,120]} |AF(90,\phi) - Desired(90,\phi)|$
Here, fig. 5.2, 5.3 & 5.4 presents the optimised simulation result for DE, SSO and both respectively. The radiation pattern of DE and SSO is compared in fig. 5.4a which shows that SSO provide more closer and smoother pattern than DE for the desired India-shaped pattern. It is observed from fig. 5.4b that the cost function of DE gets saturated after about 1500 iterations while

that for SSO gets saturated after only 500 iterations. Thus, it can be concluded that the convergence rate for SSO is much higher than that of DE. Further, it can be clearly observed from fig. 5.4c that both DE and SSO are in close proximity to the desired radiation pattern with good amount of accuracy.

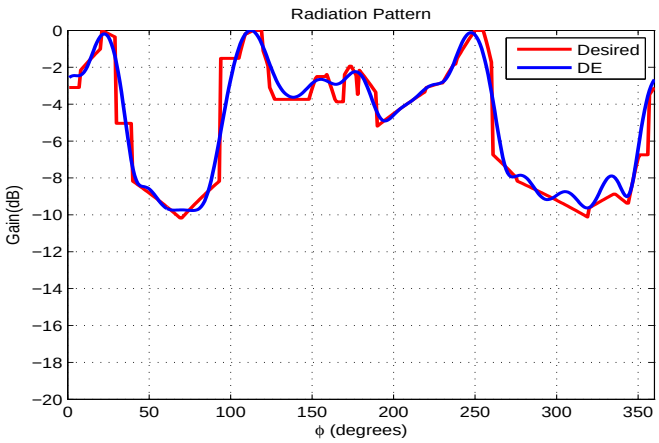

(a) 2D Radiation Pattern

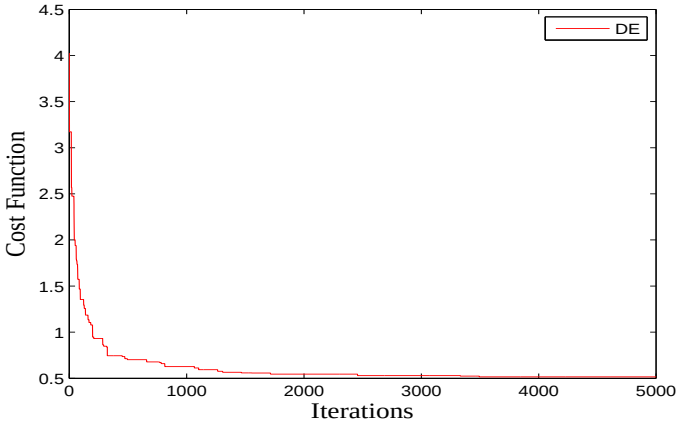

(b) Cost Function

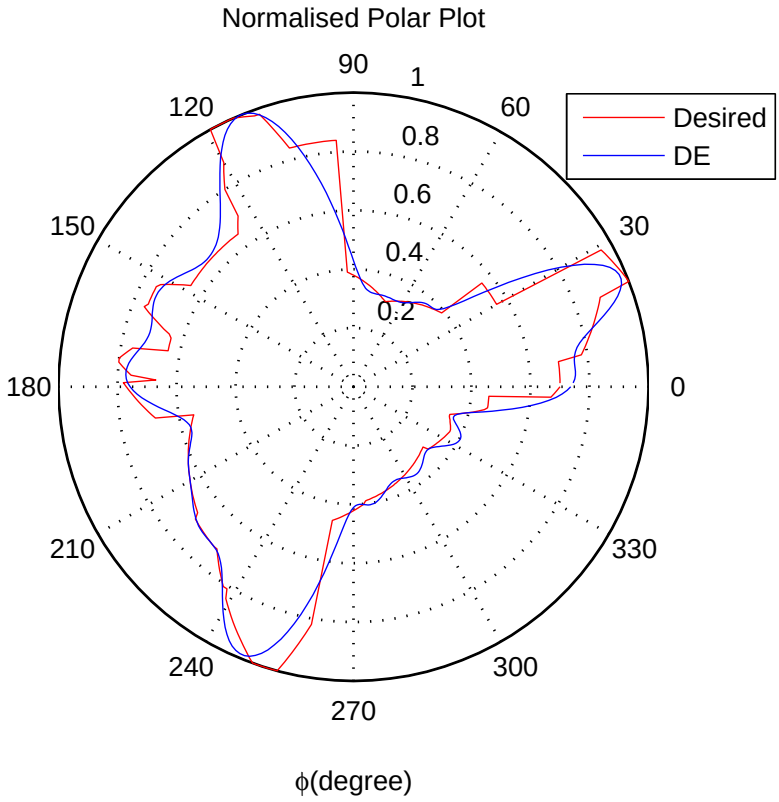

(c) Polar Radiation Pattern

Figure 5.2: India-Shaped Radiation Pattern with DE

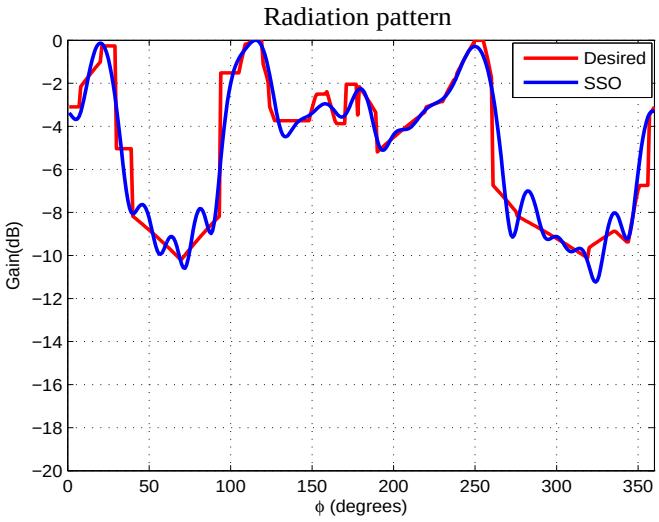

(a) 2D Radiation Pattern

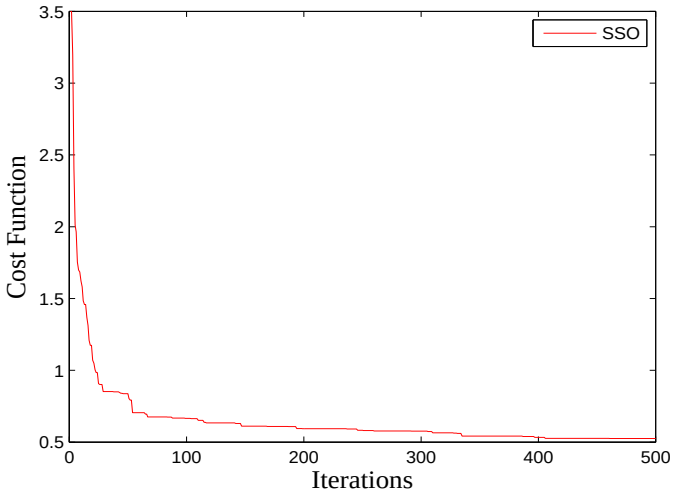

(b) Cost Function

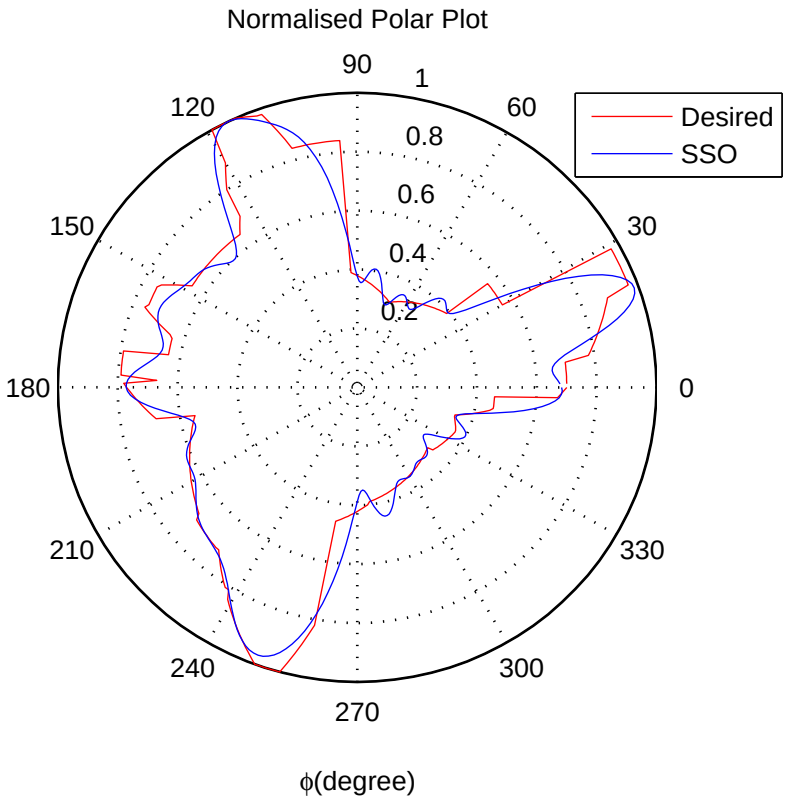

(c) Polar Radiation Pattern

Figure 5.3: India-Shaped Radiation Pattern with SSO

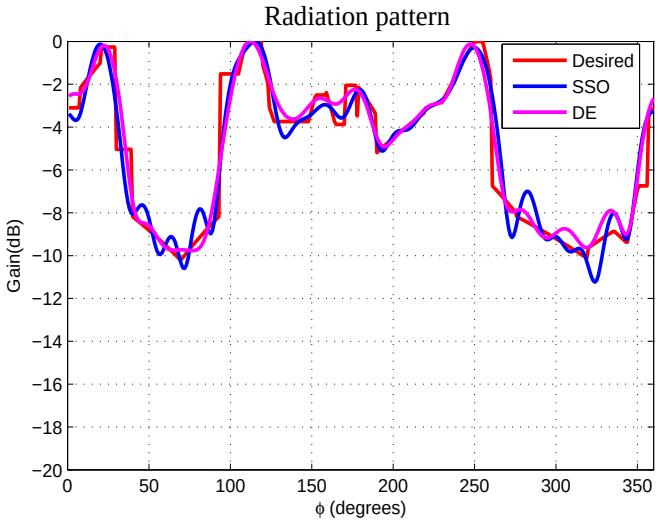

(a) 2D Radiation Pattern

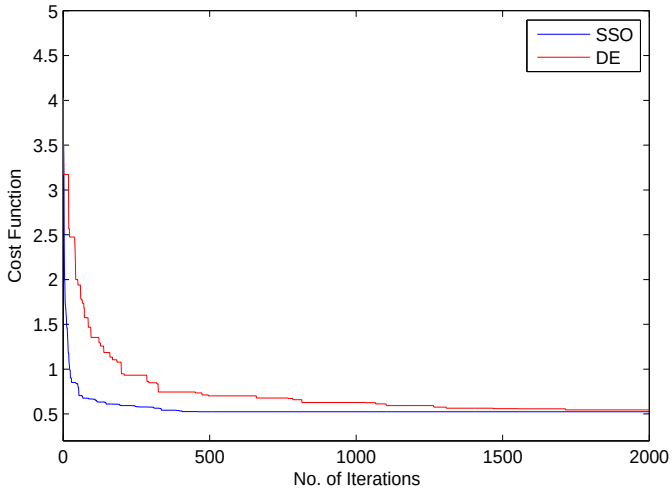

(b) Cost Function

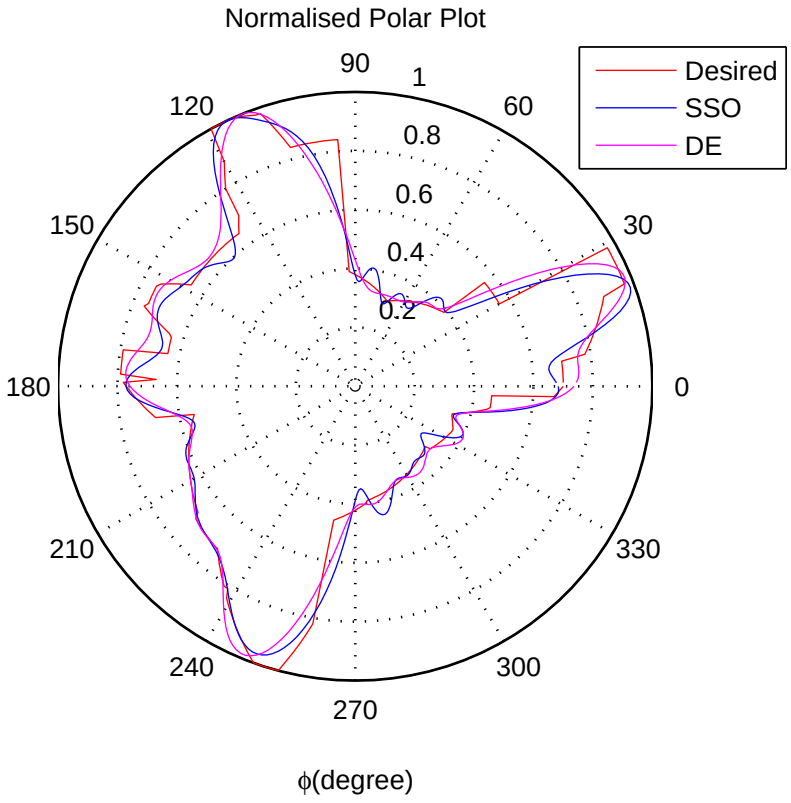

(c) Polar Radiation Pattern

Figure 5.4: India-Shaped Radiation Pattern with DE & SSO

Chapter 6

Implementation in CST Software

Computer Simulation Technology(CST) is a software tool to create the mathematical models of the physical processes and study its behaviours in computer based environment. The software actually creates mathematical equation of the approximated physical process showing the behaviour of the model at the boundary and at the beginning of the simulation. It can be used to design electromagnetic models by four different simulation techniques namely Transient solver(TS), Frequency domain solver(DMS), Integral equation solver(IES) and Eigenmode solver(ES) can be applied depending on the requirements and complexities. Here, antenna array prototype is modelled and simulated with Transient solver(TS) to analyse their behaviours and have an overview of their performance in real environmental condions.

In this section, spherical models using strip dipoles and patch dipoles have been designed in T-solver of CST software. The patch dipole of thickness(h) 2mm follows [18] for its shape and dimensions. A substrate material of low dielectric constant(ϵ_r) has been used in order to reduce the losses in the metal.

6.1 Modelling of Patch & Strip Dipole

The dimension of patch dipoles [18] depends on frequency of operation and are designed according to the mentioned equations as below:

$$\lambda_0 = \frac{c}{f}$$

Guide wavelength,

$$\lambda_d = \frac{\lambda_0}{\sqrt{\epsilon_r}}$$

$$p = \log\left(\frac{\lambda_d}{0.1016 * \lambda_0}\right) - 1$$

Width of the patch,

$$W = h * \lambda_d * p$$

Strip-width,

$$w_s = \sqrt{W}$$

$$U = \frac{w_s}{h}$$

Effective dielectric constant,

$$\epsilon_{ef} = \frac{\epsilon_r + 1}{2} + \frac{\epsilon_r - 1}{2}[1 + \frac{10}{U}]^a b$$

where,

$$a = 1 + \frac{1}{49}\ln[\frac{U^4 + (U/52)^2}{U^4 + 0.432}] + \frac{1}{18.7}\ln\frac{U}{81}^3$$

$$b = 0.564[\frac{\epsilon_r - 0.9}{\epsilon_r + 0.3}]^{0.053}$$

Effective change in length due to effective dielectric constant,

$$\Delta L = 0.412 * h\frac{\epsilon_r + 0.3}{\epsilon_r - 0.258}\frac{w_s/h + 0.264}{w_s/h + 0.813}$$

Length of patch dipole,

$$L = (\frac{c}{2f * \sqrt{\epsilon_{ef}}}) - 2\Delta L$$

Width of patch dipole,

$$W = L/3$$

Based on the above formulae, patch dipole is designed at a frequency of 2.4GHz with Teflon (ϵ_r=2.1) as substrate material. The dimensions of CST model of patch dipole referred [18] is shown in the fig.6.1. The CST design of patch dipole with its radiation pattern and S11 parameter are shown in fig 6.2. The results clearly shows that radiation pattern resembles with dipole radiation pattern with minimum losses occurring at 2.8GHz in place of 2.4GHz.

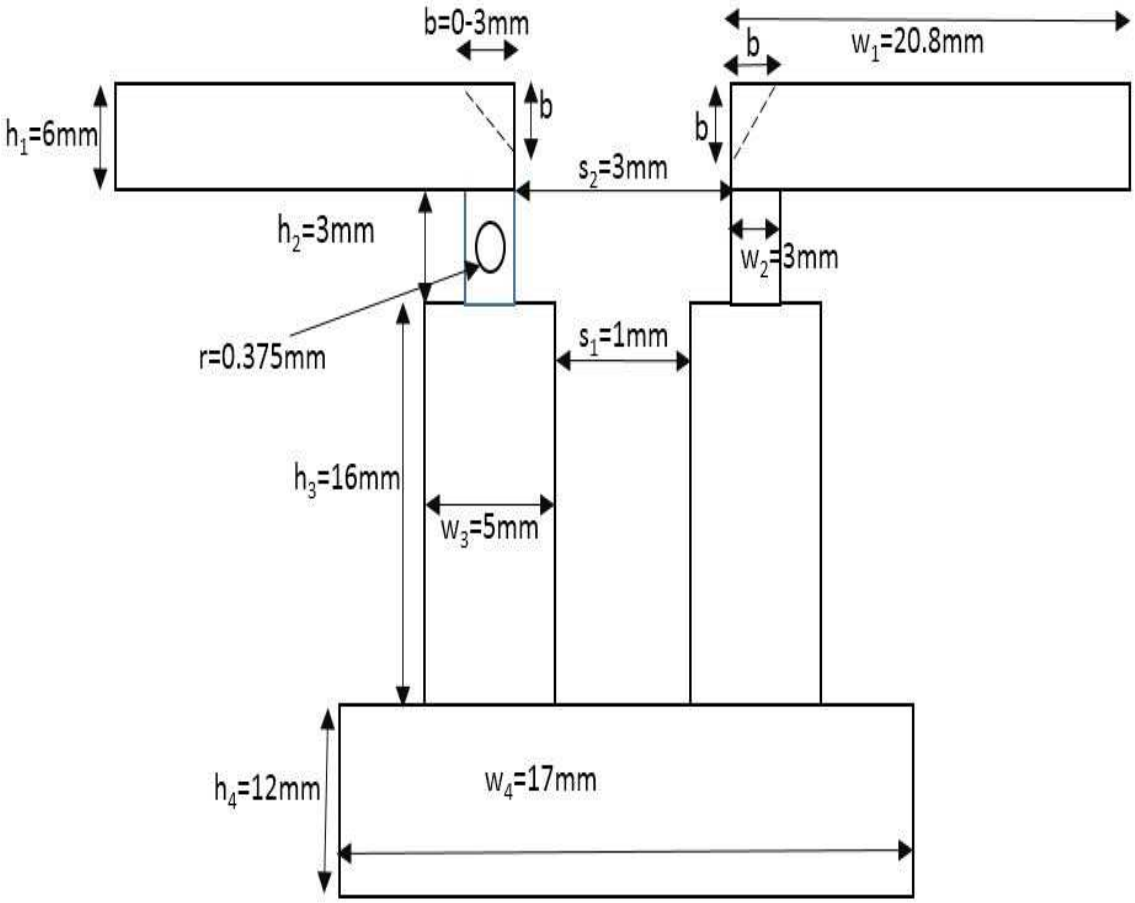

Figure 6.1: CST Patch Design at 2.4GHz

To improve the efficiency of patch at 2.4GHz, a strip dipole is designed with same material. The design of a strip dipole, its radiation pattern and S11 result as shown in fig. 6.3 clearly indicates that strip dipole has notch occurring at 2.4GHz, thereby minimum losses occurs in strip dipole at the desired operating frequency.

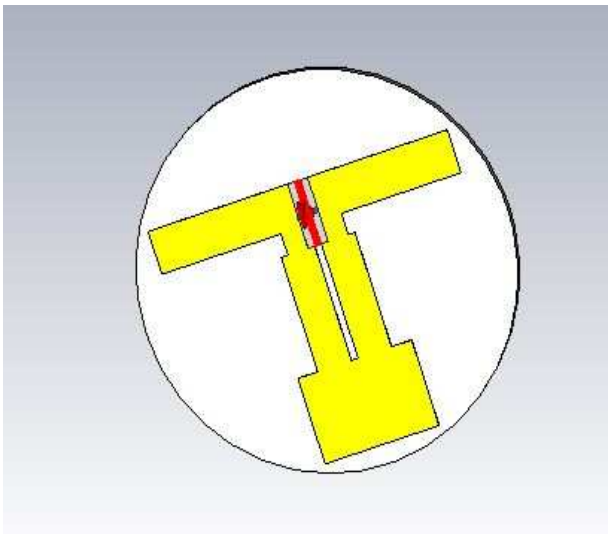

(a) Front View of Patch Dipole

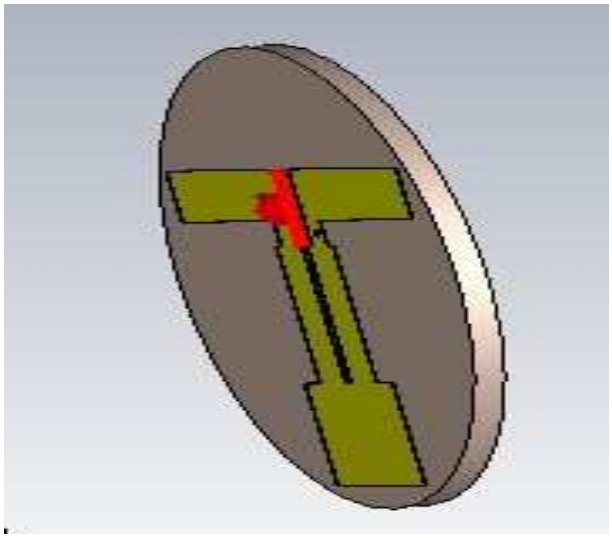

(b) Side View of Patch Dipole

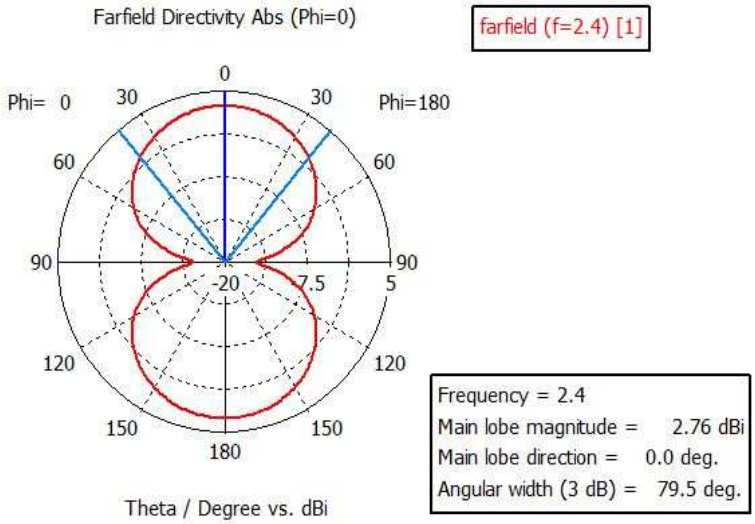

(c) Polar Pattern of Patch Dipole

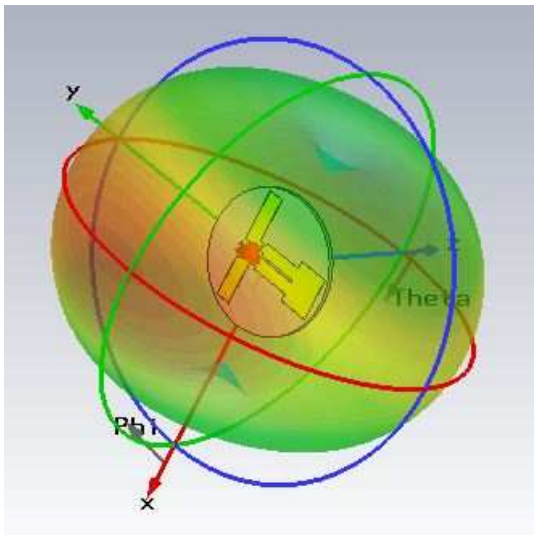

(d) 3D Pattern of Patch Dipole

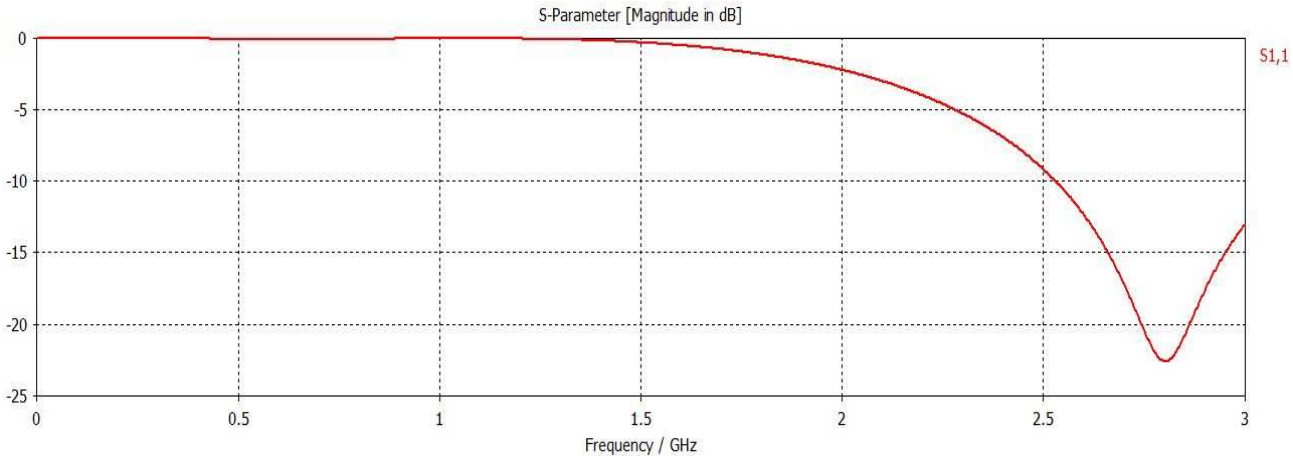

(e) S11 of Patch Dipole

Figure 6.2: Design & Radiation Pattern of Patch Dipole

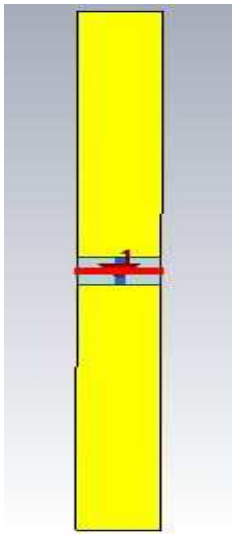

(a) Front View of Strip Dipole

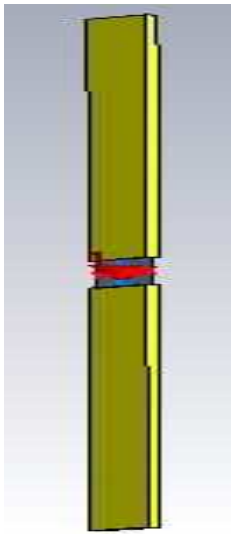

(b) Side View of Strip Dipole

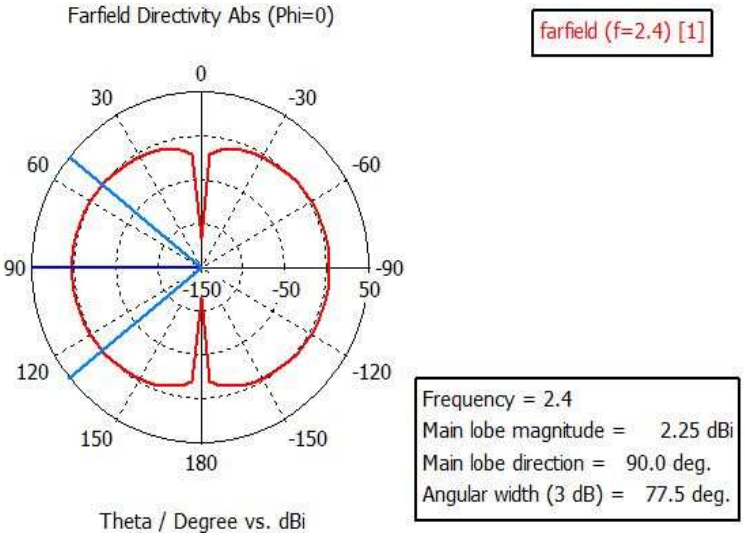

(c) Polar Pattern of Strip Dipole

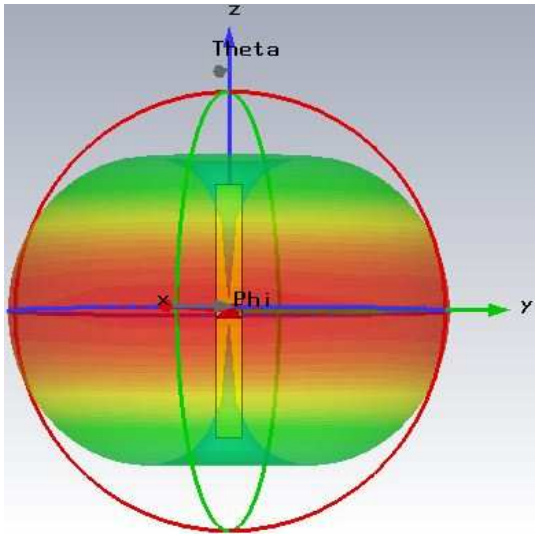

(d) 3D Pattern of Strip Dipole

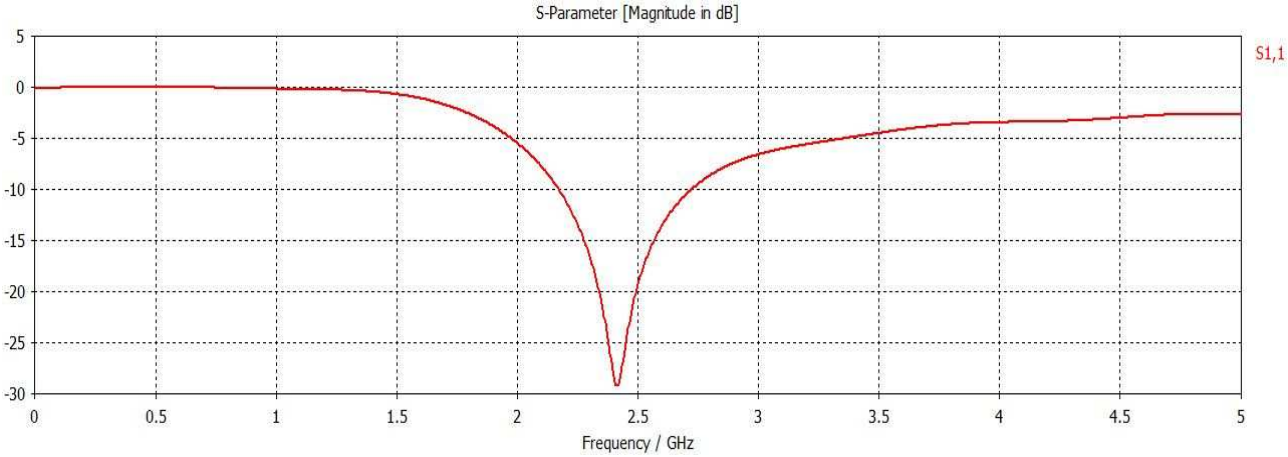

(e) S11 of Strip Dipole

Figure 6.3: Design & Radiation Pattern of Strip Dipole

6.2 Modelling of Spherical Array

Spherical Antenna Array with N=14 & N=18 antenna elements is modelled using patch and strip dipoles at a frequency of 2.4GHz with Teflon as substrate material. Fig. 6.4 & 6.5 shows the CST models, their radiation pattern and S11 parameter of spherical array with 14 & 18 patch dipole elements. It is observed from the polar plots that pattern is omni-directional in nature with good value of directivity. Also, a dip is observed in S-parameter at a frequency of 2.4GHz showing minimum reflection at desired frequency of operation. Further, going for the CST models of spherical array with strip dipole 6.6 & 6.7 for 14 & 18 elements, it can be seen that the radiation pattern becomes more smoother and regular in shape with a better value of far-field directivity specifically for N=18 elements. On the other hand, S11 parameter is moving towards lower value of frequency and the dip is observed at 2.2GHz, thereby it can be concluded that the efficiency of strip dipole spherical array decreases with increase in reflection losses. It can be further observed that the directivity keeps on increasing with increase in number of antenna elements.

Validation of CST Results with MATLAB results To validate the CST design of spherical array, it is compared with MATLAB simulation result for same number of elements as shown in fig. 6.8 & 6.9. From the results, it can be clearly observed that CST results show good approximation to MATLAB results in terms of shape of the radiation pattern for both polar and 2D-plot. It is observed from the CST and MATLAB based results that proposed array is radiating in every direction with almost similar variations in their radiation pattern. Thus, we can easily conclude from the above CST results that, spherical array can be effectively utilized in applications where approximate omni-directional pattern is required.

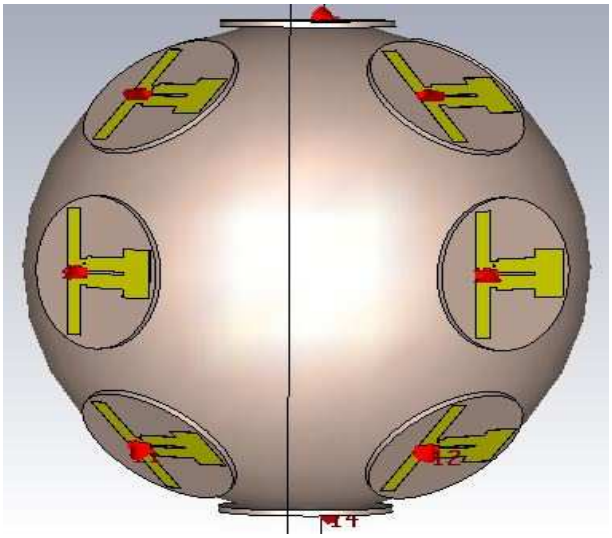

(a) Front View of Spherical Array

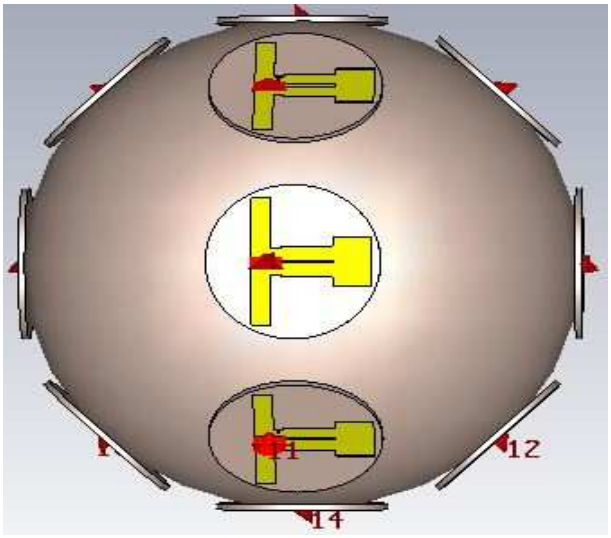

(b) Side View of Spherical Array

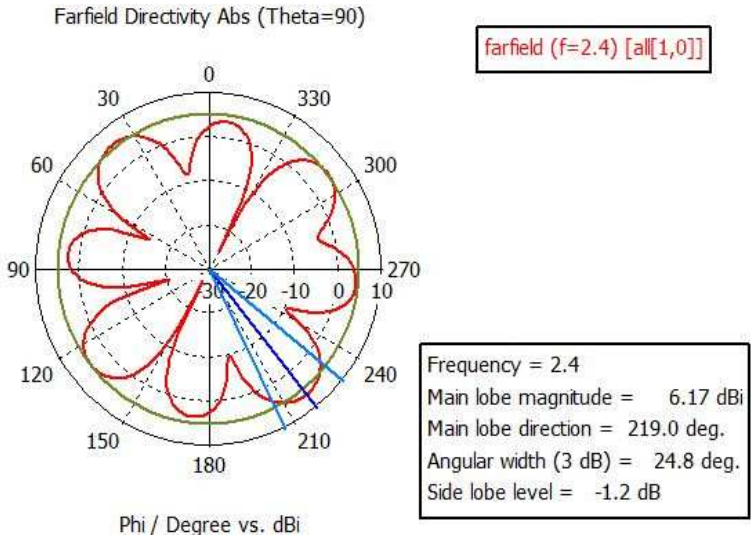

(c) Polar Pattern of Spherical Array

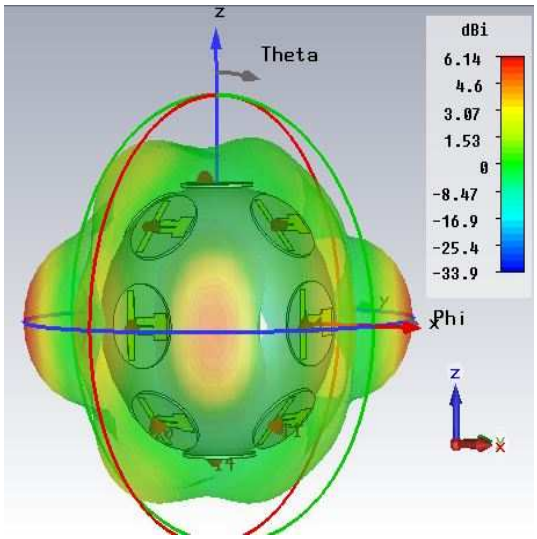

(d) 3D Pattern of Spherical Array

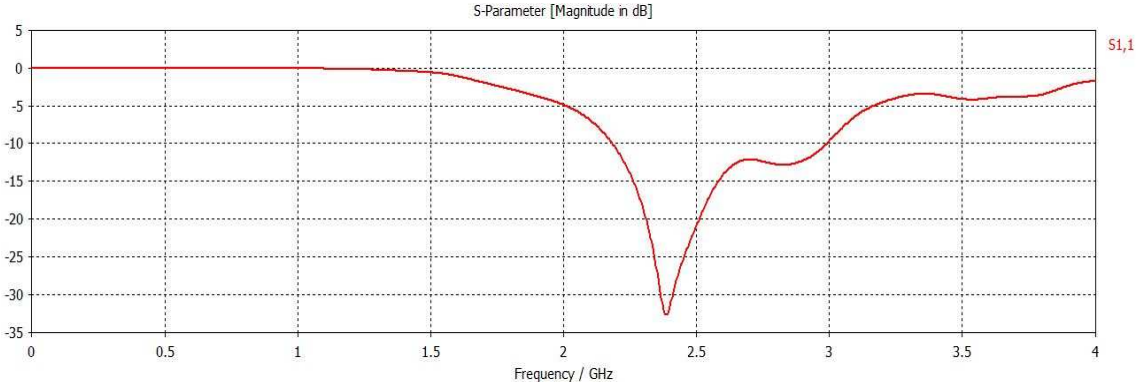

(e) S11 of Spherical Array

Figure 6.4: Design & Radiation Pattern with N=14 Patch Spherical Array

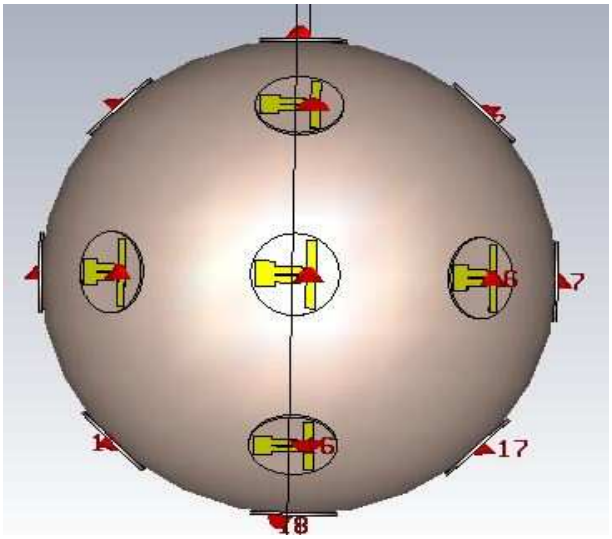

(a) Front View of Spherical Array

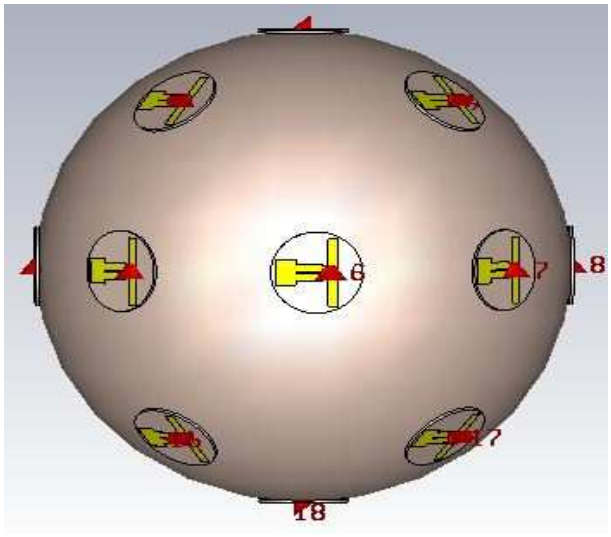

(b) Side View of Spherical Array

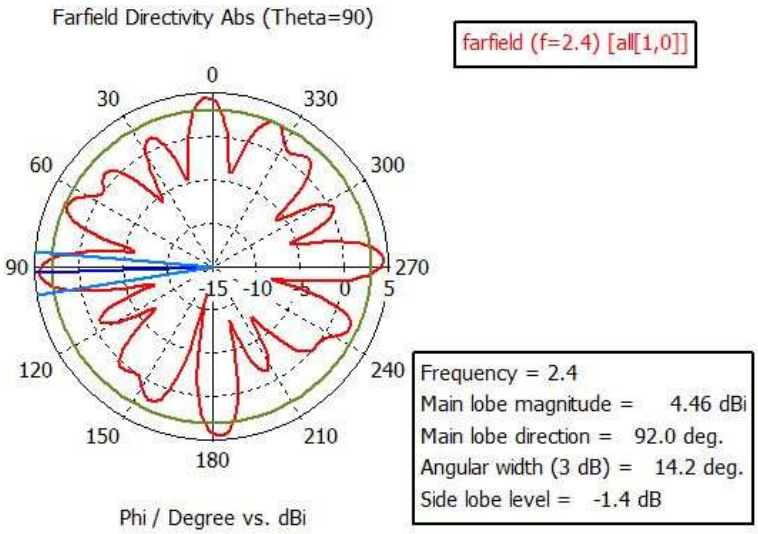

(c) Polar Pattern of Spherical Array

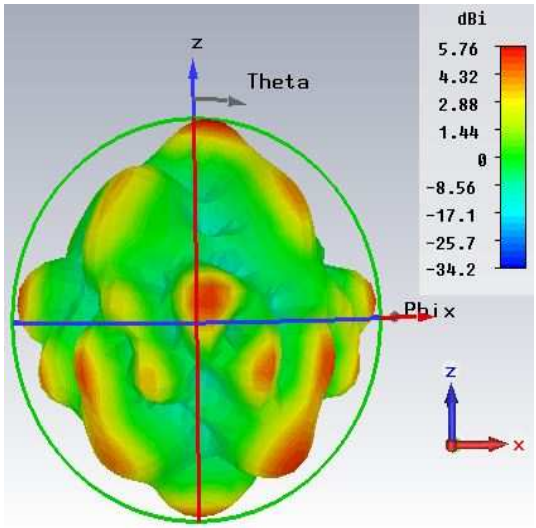

(d) 3D Pattern of Spherical Array

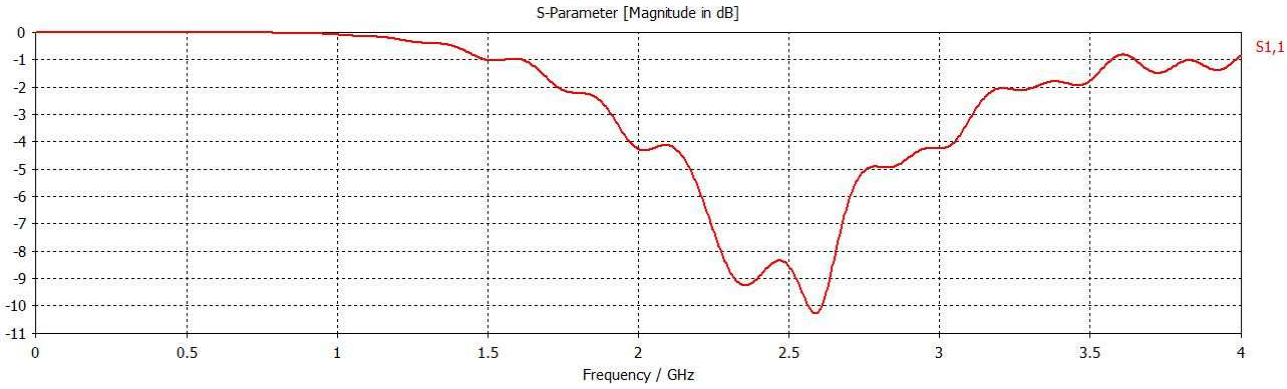

(e) S11 of Spherical Array

Figure 6.5: Design & Radiation Pattern with N=18 Patch Spherical Array

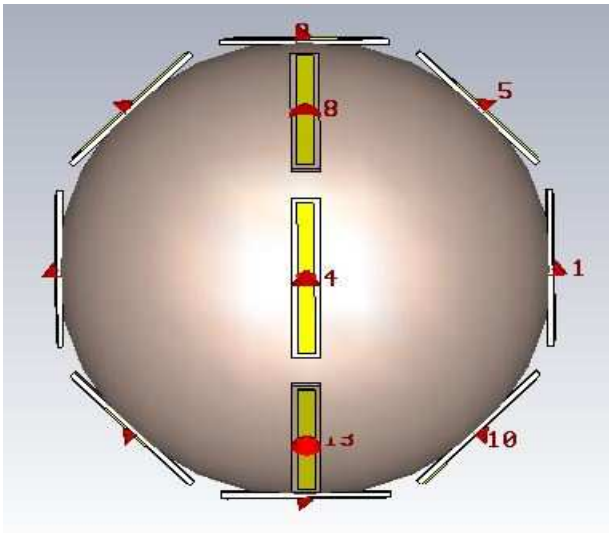

(a) Front View of Spherical Array

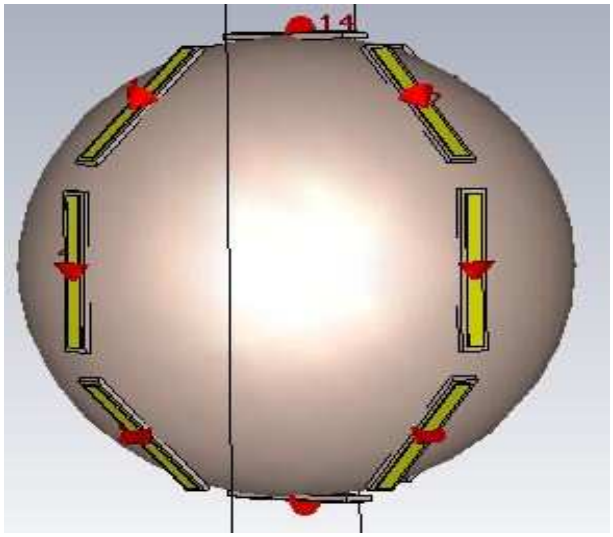

(b) Side View of Spherical Array

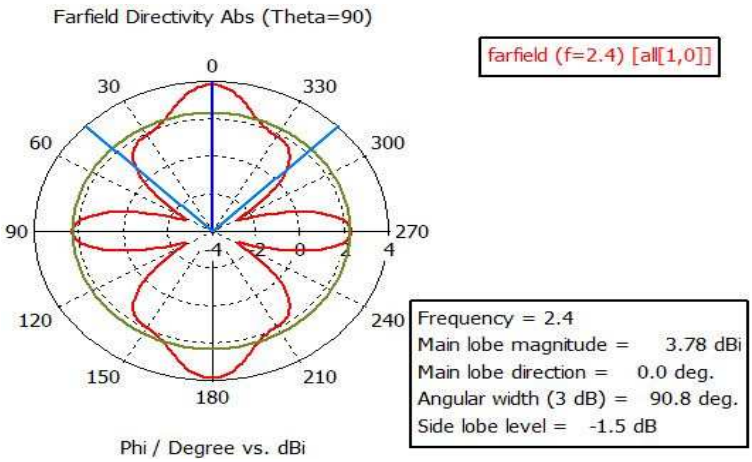

(c) Polar Pattern of Spherical Array

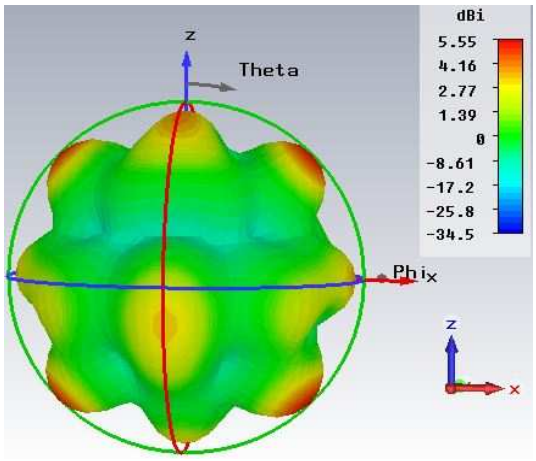

(d) 3D Pattern of Spherical Array

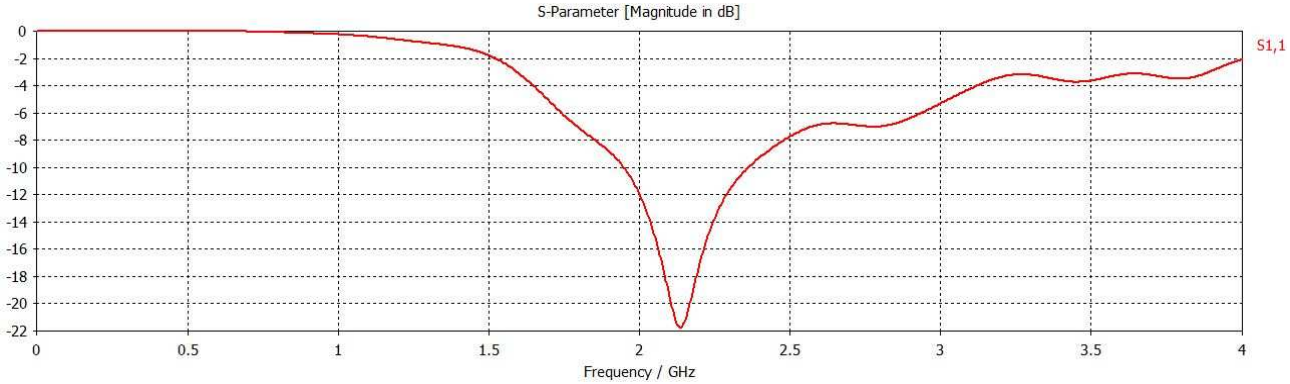

(e) S11 of Spherical Array

Figure 6.6: Design & Radiation Pattern with N=14 Strip Spherical Array

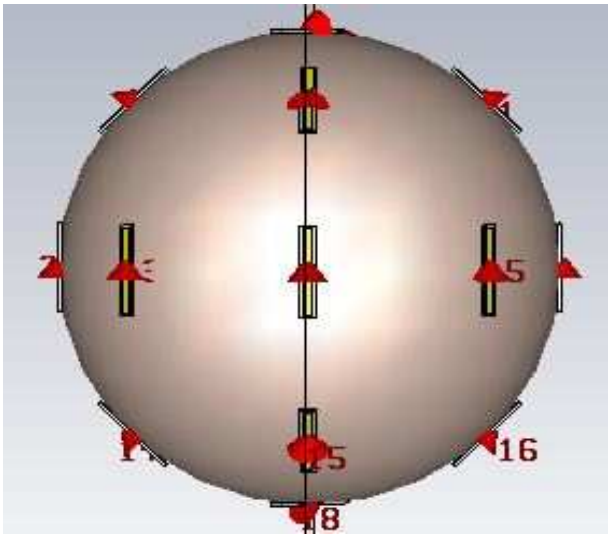

(a) Front View of Spherical Array

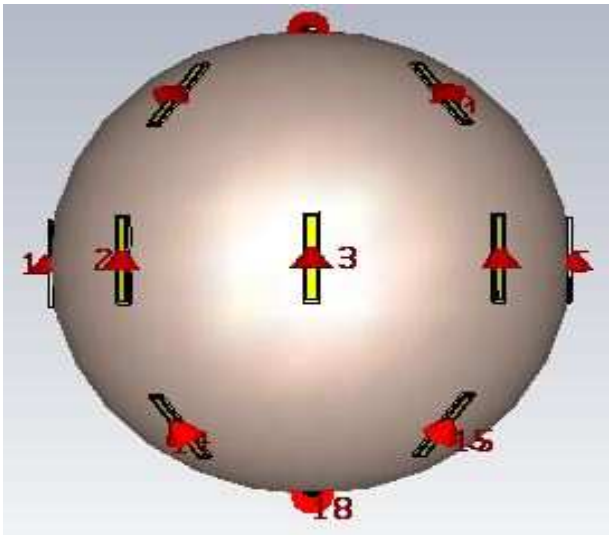

(b) Side View of Spherical Array

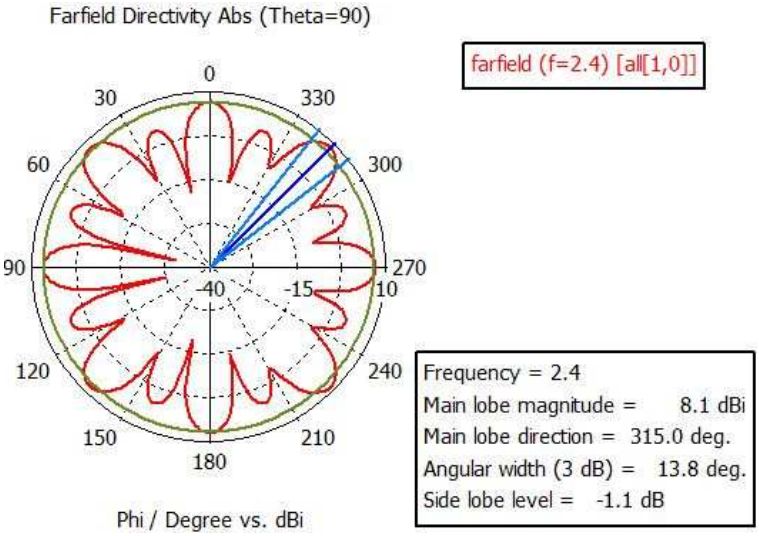

(c) Polar Pattern of Spherical Array

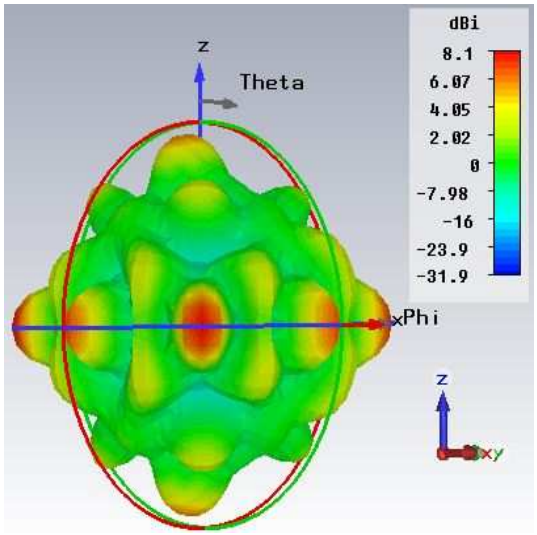

(d) 3D Pattern of Spherical Array

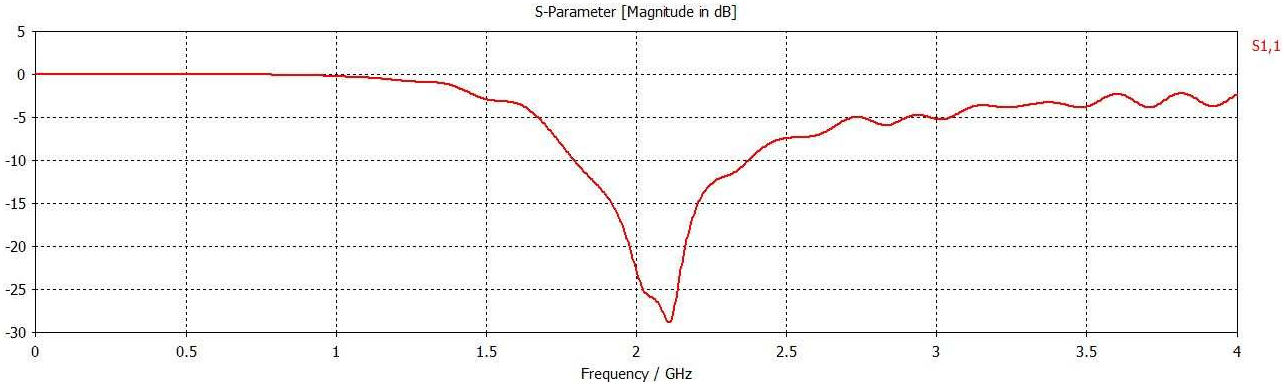

(e) S11 of Spherical Array

Figure 6.7: Design & Radiation Pattern with N=14 Strip Spherical Array

6.3 Validation of CST Results with Matlab Results

6.3.1 Working With 14 Elements Spherical Array

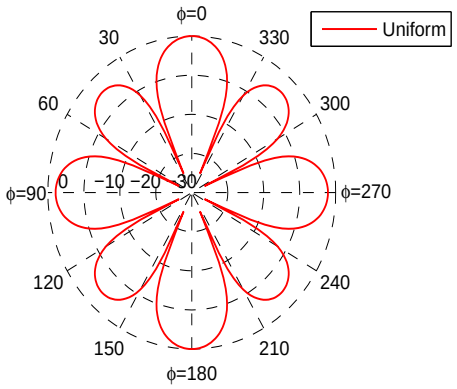

(a) MATLAB Polar Plot Spherical Array

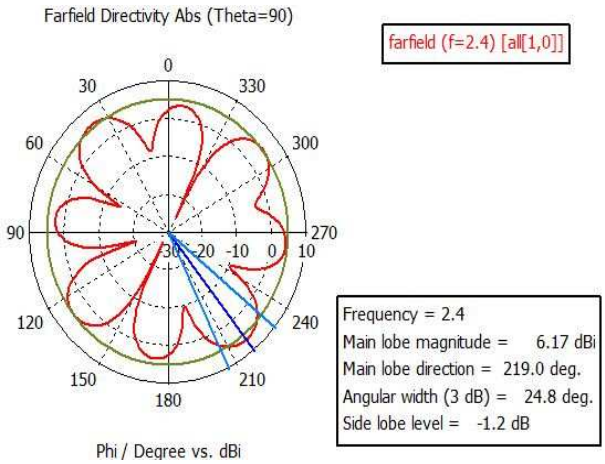

(b) CST Polar Plot Spherical Array

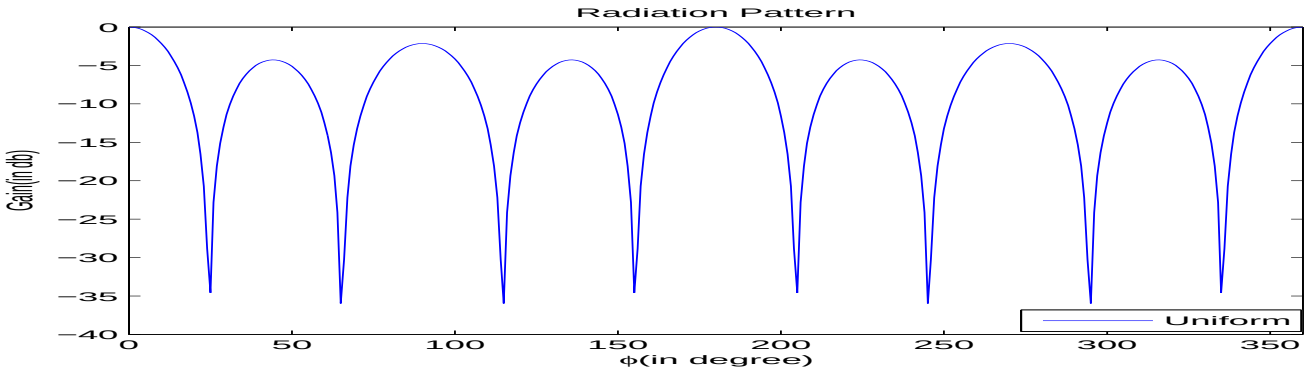

(c) 2D MATLAB Pattern of Spherical Array

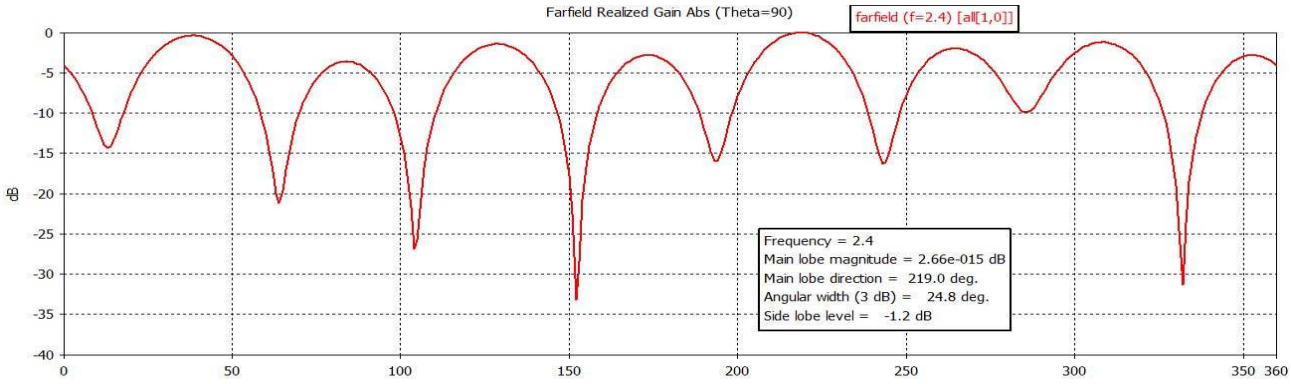

(d) 2D CST Pattern of Spherical Array

Figure 6.8: Validation with N=14 Patch Spherical Array

6.3.2 Working With 18 Elements Spherical Array

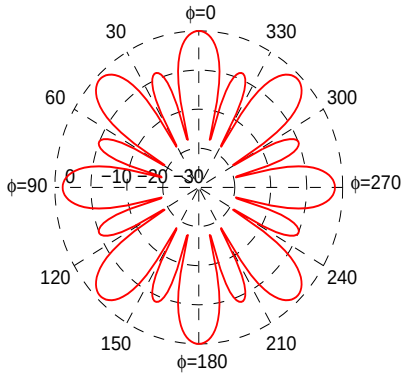

(a) MATLAB Polar Plot Spherical Array

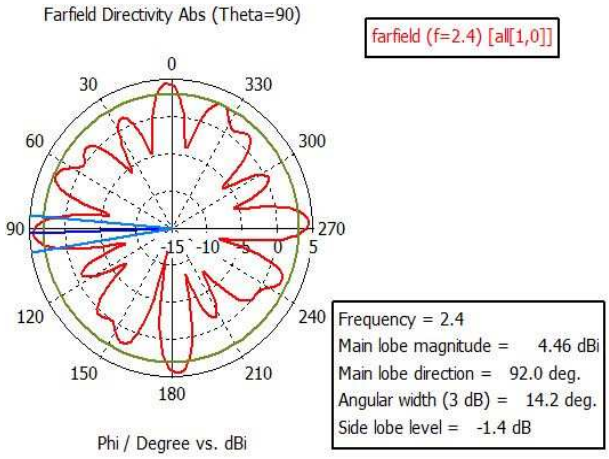

(b) CST Polar Plot Spherical Array

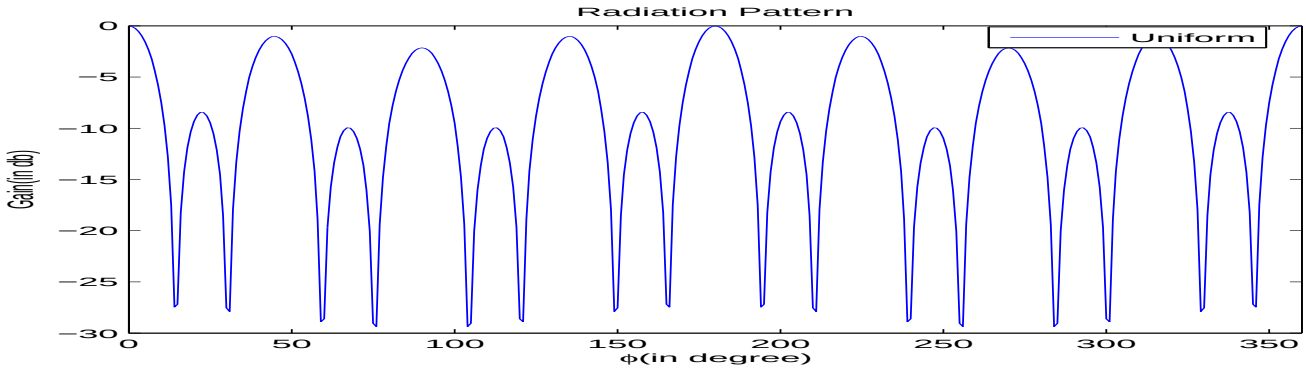

(c) 2D MATLAB Pattern of Spherical Array

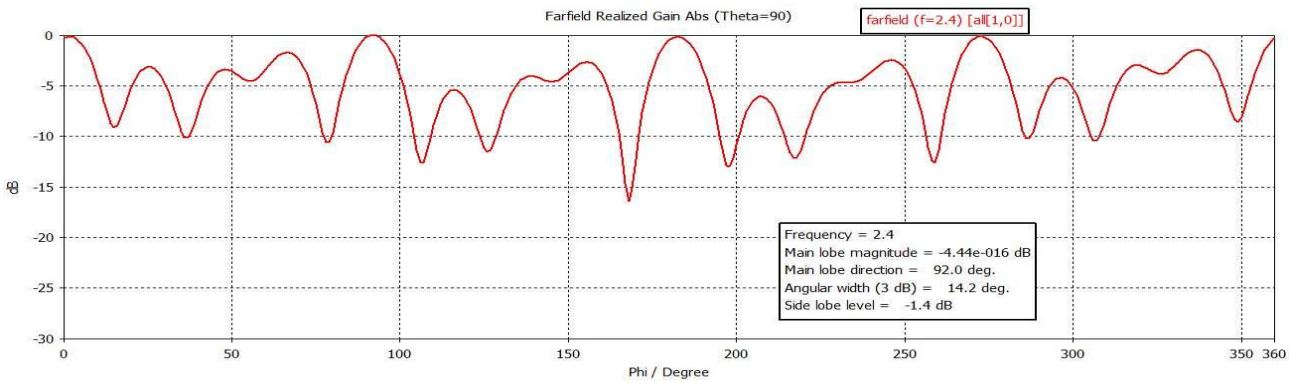

(d) 2D CST Pattern of Spherical Array

Figure 6.9: Validation with N=18 Patch Spherical Array

Chapter 7

Conclusion and Future Scope

Spherical Array Antenna offers fast electronic beam-steering, supports multi-beam radiation patterns and adaptive pattern reshaping due to their robust design and omni-directional nature of radiation pattern. These antenna array provide wide angle coverage which is difficult to achieve with planar arrays as they suffers from pattern degradation when the beam is steered off bore-sight. The following conclusions can be drawn from the simulation results of the proposed array:

7.1 Conclusions

- Conformal shape like Spherical Array can be modelled and formulated with the concept of basic conventional arrays(Linear, Planar & Circular arrays).

- Mutual coupling has tremendous impact on the radiation pattern of antenna array. While Planar array show radiation pattern variation both in magnitude and shape, linear and spherical array shows only in case of magnitude. In case of circular array, no any effect is observed, since all elements sees the same environment.

- Linear, Circular & Spherical array support Cosecant-squared shaped pattern after application of DE and SSO based optimization techniques. However, spherical array proves its superiority over linear and circular array both in terms of SLL and amount of ripples.

- Spherical arrays can be used to generates complex and typical shaped radiation patterns like India contour with much less complexity.

- Analyzed results, concludes that SSO is a better technique over DE based on the computational time and parametric complexity of the algorithm

- Spherical array is modelled using CST software and comparaed with MATLAB simulation result.

7.2 Limitations

- Proposed Spherical Array is modelled such that the array as a whole is symmetric both in azimuthal and elevation direction, but its antenna elements are symmetrically placed considering only azimuthal angle.

- Computation of Mutual Coupling is done with identical and electrically small size antenna elements oriented in same direction and excited by same current source. Further, atmospheric interferences are not taken into consideration during computation of mutual coupling.

- Isotropic Antenna elements which are theoretical are used in the generation of Cosecant-squared shaped and proposed India-shaped radiation pattern.

- Standard DE & SSO algorithms are applied for optimization to generate the desired patterns.

7.3 Future Scope

- A completely symmetric spherical array can be modelled and formulated so that element-wise symmetry can be achieved and perfect omnidirectional pattern can be generated.

- Discussed Shaped patterns can be generated using practical antenna as radiating element in the proposed spherical array.

- Highly efficient and latest Neuro-Fuzzy tools can be utilized to generate more accurate results.

- The work can be extended to other complex shaped radiation patterns .

Bibliography

[1] Lars Josefsson and Patrik Persson. *Conformal array antenna theory and design*, volume 29. John wiley & sons, 2006.

[2] Constantine A Balanis. *Antenna theory: analysis and design*. Wiley-Interscience, 2012.

[3] Xiao-Ding Cai and GI Costache. Numerical analysis of mutual coupling effects in linear and circular arrays. In *Antennas and Propagation Society International Symposium, 1992. AP-S. 1992 Digest. Held in Conjuction with: URSI Radio Science Meeting and Nuclear EMP Meeting., IEEE*, pages 641–644. IEEE, 1992.

[4] Thomas Svantesson. Modeling and estimation of mutual coupling in a uniform linear array of dipoles. In *Acoustics, Speech, and Signal Processing, 1999. Proceedings., 1999 IEEE International Conference on*, volume 5, pages 2961–2964. IEEE, 1999.

[5] David F Kelley and Warren L Stutzman. Array antenna pattern modeling methods that include mutual coupling effects. *Antennas and Propagation, IEEE Transactions on*, 41(12):1625–1632, 1993.

[6] Simon Henault, Symon K Podilchak, Said M Mikki, and Yahia MM Antar. A methodology for mutual coupling estimation and compensation in antennas. *Antennas and Propagation, IEEE Transactions on*, 61(3):1119–1131, 2013.

[7] Xiao Peng and Feng Zhenghe. A pattern synthesis method for linear array considering mutual coupling effect. In *Microwave and Millimeter Wave Technology, 2002. Proceedings. ICMMT 2002. 2002 3rd International Conference on*, pages 676–680. IEEE, 2002.

[8] Xiao-Miao Zhang, Kwai Man Luk, Qing-Feng Wu, Tao Ying, Xue Bai, and Liang Pu. Cosecant-square pattern synthesis with particle swarm optimization for nonuniformly spaced linear array antennas. In *2008 8th International Symposium on Antennas, Propagation and EM Theory*, pages 193–196, 2008.

[9] Debasis Mandal and AK Bhattacharjee. Synthesis of cosec 2 pattern of circular array antenna using genetic algorithm. In *Communications, Devices and Intelligent Systems (CODIS), 2012 International Conference on*, pages 546–548. IEEE, 2012.

[10] Ananda Kumar Behera, Aamir Ahmad, SK Mandal, GK Mahanti, and Rowdra Ghatak. Synthesis of cosecant squared pattern in linear antenna arrays using differential evolution. In *Information & Communication Technologies (ICT), 2013 IEEE Conference on*, pages 1025–1028. IEEE, 2013.

[11] Jason Brownlee. *Clever Algorithms: Nature-Inspired Programming Recipes*. Jason Brownlee, 2011.

[12] Rainer Storn and Kenneth Price. Differential evolution - a simple and efficient adaptive scheme for global optimization over continuous spaces. *Technical Report TR-95-012*, March 1995.

[13] Swagatam Das and Ponnuthurai Nagaratnam Suganthan. Differential evolution: A survey of the state-of-the-art. *Evolutionary Computation, IEEE Transactions on*, 15(1):4–31, 2011.

[14] Rainer Storn. On the usage of differential evolution for function optimization. *NAFIPS*, pages 519–523, 1996.

[15] Changseok Bae, Wei-Chang Yeh, Noorhaniza Wahid, Yuk Ying Chung, and Yao Liu. A new simplified swarm optimization (sso) using exchange local search scheme. *International Journal of Innovative Computing, Information and Control*, 8(6):4391–4406, 2012.

[16] S Revathi and A Malathi. Network intrusion detection using hybrid simplified swarm optimization and random forest algorithm on nsl-kdd dataset.

[17] Majid M Khodier and Mohammad Al-Aqeel. Linear and circular array optimization: A study using particle swarm intelligence. *Progress In Electromagnetics Research B*, 15:347–373, 2009.

[18] Constantinos Votis, Vasilis Christofilakis, and Panos Kostarakis. Geometry aspects and experimental results of a printed dipole antenna. *International Journal Communications, Net-work and System Sciences*, 3(2):97–100, 2010.

[19] Robert S.Elliott. *ANTENNA THEORY AND DESIGN*. John Wiley and Sons, Ltd, 2005.

[20] Rainer Storn and Kenneth Price. Differential evolution a simple evolution strategy for fast optimization. *Dr. Dobb's*, (03):1824 and 78, April 1997.

[21] Thanathip Sum-Im. A novel differential evolution algorithmic approach to transmission expansion planning. 2009.

Authors Biography

ARPIT KUMAR BARANWAL was born to Mr. Vijay Kumar Baranwal and Mrs. Seema Baranwal on 25th Feb, 1990 at Mau District, Uttar Pradesh, India. He obtained Bachelor's degree in Electronics and Communication Engineering from K.N. Modi Institute of Engineering and Technology , Modinagar(Gzb), Uttar Pradesh in 2011. He joined the Department of Electrical Engineering, National Institute of Technology, Rourkela in July 2012 as an Institute Research Scholar to pursue M.Tech degree in "Electronics System and Communication" specialization.